

A Tale of Two Imperatives: Privacy and Explainability

Supriya Manna
SRM University AP

REACHSMANNA@GMAIL.COM

Niladri Sett
Data Science Lab, SRM University AP

SETTNILADRI@GMAIL.COM

Abstract

Deep learning's preponderance across scientific domains has reshaped high-stakes decision-making, making it essential to follow rigorous operational frameworks that include both Right-to-Privacy (RTP) and Right-to-Explanation (RTE). This paper examines the complexities of combining these two requirements. For RTP, we focus on 'Differential privacy' (DP), which is considered the current *gold standard* for privacy-preserving machine learning due to its strong quantitative guarantee of privacy. For RTE, we focus on post-hoc explainers: they are the *go-to* option for model auditing as they operate independently of model training. We formally investigate DP models and various commonly-used post-hoc explainers: how to evaluate these explainers subject to RTP, and analyze the intrinsic interactions between DP models and these explainers. Furthermore, our work throws light on how RTP and RTE can be effectively combined in high-stakes applications. Our study concludes by outlining an industrial software pipeline, with the example of a wildly used use-case, that respects both RTP and RTE requirements.

1 Introduction

Deep learning has achieved massive success over the past decade in several domains and high stakes Dong et al. (2021). It has been a cornerstone ever since in almost all aspects of scientific discoveries. However, it is to be noted that deep learning, although predominant in today's scientific understandings, comes with its inherent shortcomings Talaei Khoei et al. (2023); Saeed and Omlin (2023); Boulemtafes et al. (2020). In this paper, we shall investigate the intricacies of two such pivotal shortcomings: **Privacy** and **Explainability**. We shall thereafter substantiate our findings with a famous use case from previous studies.

Firstly, the deep models, although achieve superior performance across domains, are inherently prone to sensitive data leakage Boulemtafes et al. (2020). It has been extensively shown that the models can leak information about the data with which it has been trained. Even, especially in the biomedical domain, it has been shown that simple 'linkage' attacks can exploit anonymized electronic health records Sweeney (2015). Due to the inherently vulnerable nature of deep models, it is not only prone to severe privacy attacks including membership inference (MIA) Hu et al. (2022), model stealing Oliynyk et al. (2023), model inversion Fredrikson et al. (2015); Wang et al. (2021); Veale et al. (2018) etc but also impose a threat on the applicability of deep learning in real-world applications.

Secondly, the deep models are *hard* to explain Saeed and Omlin (2023). Neural nets are nonlinear systems, often try to learn the (approximate) distribution of the training data.

However, once a model is deployed in an *open-world* setting Zhu et al. (2024), there is no gold label to cross-check the prediction obtained as a result, the subtle notion of *trust* on the prediction is pivotal to move forward with the same. But as these models are excessively critical, how did the model come to the prediction is a non-trivial phenomenon Jentzen et al. (2023).

To tackle the first problem, researchers have developed several strategies for privacy-preserving machine learning Boulemtafes et al. (2020). This includes homomorphic encryption Pulido-Gaytan et al. (2020), PATE Papernot et al. (2018), differential privacy (DP) Abadi et al. (2016) etc; depending on the setting and motivation we incorporate these methods to make the model *robust* against diverse privacy attacks. However, differential privacy (DP), over the years, has been established as a *gold-standard* for privacy-preserving machine learning Blanco-Justicia et al. (2022); Suriyakumar et al. (2021) mainly due to its *worst case guarantee* against *any* inference attacks Abadi et al. (2016); Dwork et al. (2014). Furthermore, other types of privacy attacks are not as mature and/or successful as MIA is Rigaki and Garcia (2023). In this paper, we have specifically worked on DP models¹ with diverse *privacy guarantees* aka ϵ Dwork et al. (2014).

On the other hand, to tackle the explainability problem, researchers have developed an array of methods to audit the model decisions Rudin et al. (2021); Saeed and Omlin (2023). This includes (but not limited to) local Ribeiro et al. (2016); Lundberg and Lee (2017); Sundararajan et al. (2017); Smilkov et al. (2017) and global explainability methods Ibrahim et al. (2019); Lundberg et al. (2020), inherently interpretable machines Molnar et al. (2020); Ditz (2024) etc. Among these, local post-hoc explainers have emerged as a popular and widely adopted tools for model auditing in recent times Saeed and Omlin (2023). Furthermore, post-hoc explainers' 'plug-and-play' nature is one of the crucial reasons for their massive success especially, in the industrial settings Bhatt et al. (2020b). In this work, we employ five popular post-hoc explainers relevant to our use case to obtain explanations.

Although privacy and explainability aspects have been vastly explored independently, there is little to no work incorporating them together. Despite the rapid advancements in AI, integrating privacy and explainability in high-stakes domains remains an unsolved and pressing challenge. Existing research has treated privacy and explainability as separate challenges, leaving a significant gap in understanding their interplay. This gap becomes critical in high-stakes applications where both are non-negotiable. Researchers in privacy-preserving machine learning have investigated several aspects of differential privacy such as the scalability of DP models Beltran et al. (2024), their fairness Fioretto et al. (2022), robustness Tursynbek et al. (2020), privacy-utility trade-off Zheng et al. (2024) etc. On the other side, researchers have worked on different aspects of explainable AI (XAI) such as faithfulness Lyu et al. (2024), robustness Sinha et al. (2021); Ivankay et al. (2022), and the quality of explanations Zhou et al. (2021) to name a few. In this paper, we take the first comprehensive step toward bridging the divide between privacy-preserving models and explainable AI in high-stakes domains. We explore the unique challenges that emerge when attempting to integrate privacy and explainability aspects in high-stakes applications. We investigate the underlying causes of these challenges, examine the trade-offs involved, and

1. Throughout the paper we use DP model(s)/explanation(s) and private model(s)/explanation(s) interchangeably.

discuss key considerations necessary for developing frameworks to successfully incorporate these two critical aspects effectively.

Integrating privacy and explainability is non-trivial, but addressing these issues is crucial for ensuring trustworthy and effective AI systems in high-stakes. In this context, we argue that it is equally important to identify use cases where achieving ‘the best of both worlds’ is not just desirable but a *requirement*. For example, if the training data is open source or an interpretable model (e.g. decision trees) is considered for the study, our research may not be well-motivated or the findings are not ‘worthy’. This is why, for this paper, we have considered the well-established use-case of disease detection from chest x-ray Al-qaness et al. (2024). The reason to choose the same is that medical records are (almost) always subject to privacy preservation and it is of paramount importance that, with explanations, the stakeholders including both physician and patients can *trust* the model predictions. Post-hoc explainers, which we use in this paper, have been extensively utilized for our chosen and similar use-cases in past Gaudio (2023); E. Ihongbe et al. (2024); Gwinner et al. (2024); Saxena et al. (2022); Ifty et al. (2024); prasad Kooyada and Singh (2023); Sarp et al. (2023).

The dual mandates of the Right-to-Privacy (RTP) Thomson (1975) and the Right-to-Explanation (RTE) Vredenburgh (2022), increasingly imposed by governments for high-stakes AI applications, underscore the urgency of addressing these intertwined imperatives. Despite their critical importance, prior research lacks a comprehensive and systematic feasibility study that explores the practical integration of these rights within AI systems. Fundamental questions remain unanswered: How should we evaluate the quality of explanations for DP models? Can existing popular local post-hoc explainers reliably function in this setting, or do they falter under the constraints of differential privacy? If they fail, what alternative methods can generate comparable private explanations? Our work makes a fundamental contribution by systematically addressing these pressing questions, providing not only foundational clarity but also actionable insights grounded in rigorous empirical analysis. Formally, our central research question in this paper is:

■ Do DP models and post-hoc explainers *go together*?

Our contributions are as follows:

- We propose the desiderata for private explanations to follow;
- We investigate the interplay between the DP models and post-hoc explainers subject to the desiderata proposed;
- We conduct extensive experiments and report our findings: we consider three types of widely used CNN models, six distinct ϵ values to train them on, and five popular post-hoc methods for our experiment;
- We present a rigorous study on the mechanistic interpretation of the DP models; depicting the interplay of the post-hoc explainers with DP models;
- We propose a novel framework that can achieve RTP and RTE together for high-stakes applications; we exemplify the same by outlining an end-to-end privacy-preserving pipeline for our use case.

The rest of the paper is organized as follows. We brief the preliminary concepts of DP and post-hoc explainers. We point out the ways an adversary can attack, followed by an extensive discussion on several quantifiable notions for explanations' quality, and their inherent shortcomings in Section 3. We formally introduce our proposed desiderata and measures to quantify explanation quality in Section 4. We detail our experimental setup in Section 5. We discuss and our findings and mechanistically interpret the models to explain our findings in Sections 6 and 7. Next, we explore Local Differential Privacy and its applicability in our context, in Section 8. We outline our privacy-preserving pipeline in Section 9. We present the related works in Section 10. Finally, we point out the limitations of our work in Section 11, and conclude in Section 12.

2 Preliminaries

Privacy-preserving machine learning is the building block for RTP in modern day ML systems. Researchers have developed numerous strategies for privacy-preserving machine learning, including homomorphic encryption, PATE, and differential privacy (DP) Boulemtafes et al. (2020); Papernot et al. (2018); Abadi et al. (2016). Among these, DP has emerged as the *gold standard* due to its strong *worst-case guarantee* against inference attacks Blanco-Justicia et al. (2022); Dwork et al. (2014). In this work, we focus on DP models with varying privacy guarantees.

A randomized mechanism \mathcal{F} satisfies (ϵ, δ) -DP if, for any two neighboring datasets D and D' differing in at most one record, and for all measurable subsets \mathcal{S} of the output space,

$$\Pr[\mathcal{F}(D) \in \mathcal{S}] \leq e^\epsilon \Pr[\mathcal{F}(D') \in \mathcal{S}] + \delta.$$

Here, δ represents the probability of the mechanism failing to provide privacy guarantees. Specifically, it accounts for the small chance that the added noise does not sufficiently obscure the presence or absence of an individual in the dataset. Smaller values of δ are preferred.

DP comes with a few interesting properties such as sequential composition, parallel composition and, post-processing. In our study, post-processing is most relevant which let the user perform arbitrary operations on the output of a DP mechanism Dwork et al. (2014).

To make a model differentially private (DP), it undergoes privacy-preserving training, with DP-SGD being the most prominent method Ponomareva et al. (2023). It introduces Gradient clipping ensuring bounded contributions of individual data points and noise to the gradients during each update to ensure differential privacy Abadi et al. (2016). Gaussian noise is commonly used due to its well-analyzed privacy guarantees. Alternatively, laplacian noise is employed in some contexts where bounded sensitivity is easier to calculate Dwork et al. (2014). For DP-SGD, gaussian noise is predominantly used whereas, Laplacian noise is popular in Local Differential Privacy (LDP) Dwork et al. (2014); Ponomareva et al. (2023).

Local Differential Privacy (LDP) provides privacy guarantees at the data source. A mechanism \mathcal{F} satisfies ϵ -LDP if, for any two inputs x and x' and all outputs y ,

$$\Pr[\mathcal{F}(x) = y] \leq e^\epsilon \Pr[\mathcal{F}(x') = y].$$

In this work, we denote the non-private model as \mathcal{M} . We obtain its private counterpart \mathcal{M}' by retraining with DP-SGD.

Explainable machine learning is crucial for Right-to-Explainability (RTE). As mentioned earlier, this paper focuses on local, post-hoc explainers (denoted as \mathcal{I}) due to their “plug-and-play” nature, which makes them highly practical, especially for industrial applications Bhatt et al. (2020b). Broadly, these explainers can be classified into two categories: Perturbation-based methods and Gradient-based methods. Both types of methods take a model (g) and a datapoint (x) as input and output a feature attribution score(s) against $g(x)$. A feature attribution score (FAS) (or a feature attribution vector) consists of scores assigned to individual features of the given input representing their importance towards the classification the given model comes up with. A positive attribution score implies a feature has positively contributed towards the classification and negative attribution score shows that a feature does not positively contribute towards the classification. Given an explainer and a datapoint (x), we denote the FAS which explains the prediction of \mathcal{M} and \mathcal{M}' as s and s' respectively; given $\mathcal{M}(x) = \mathcal{M}'(x)$.

In our use case, s (and s') are typically computed on a per-pixel or per-element basis, and they generally match the dimensions of the input or the corresponding intermediate layer. In the next section, we shall discuss the non-private setup and potential security breaches involved.

3 Two Side of the Coin: Privacy and Explainability

3.1 The Privacy Aspect

The non-private setup consists of an adversary \mathbf{A} , having access to a data-point x , a non-private model \mathcal{M} , the output vector \mathbf{V} obtained from \mathcal{M} for x , an explainer \mathcal{I} generating a feature attribution score s against $\mathcal{M}(x)$.

From the point of \mathbf{A} , we identify two distinct ways of attacking and leaking the information from the trained model²:

1. For a given data-point x , assuming \mathbf{A} has access to the output vector \mathbf{V} from the trained model \mathcal{M} , \mathbf{A} can perform an MIA on the model Hu et al. (2022).
2. Assuming \mathbf{A} has access to the feature attribution score s of x generated by \mathcal{I} subject to $\mathcal{M}(x)$, \mathbf{A} can leverage s to execute an MIA on \mathcal{M} Shokri et al. (2021), especially when \mathcal{I} is *faithful*.

However, as \mathcal{M}' , is the DP counterpart of \mathcal{M} , it inherits the post-processing property Dwork et al. (2014) which makes *any* mechanism including obtaining \mathbf{V} , s , applied over \mathcal{M}' to produce results which are also DP, so we can mitigate both of the breaches.

3.2 The Explainability Aspect

As discussed earlier, in this study we are exclusively considering local post-hoc explainers Lundberg et al. (2020); Huber et al. (2021); Lundberg and Lee (2017). The *quality* these local explanations are judged across several parameters Hedström et al. (2023): **Faithfulness**

2. As in this paper we are working with DP models, we have considered MIA as the only type of potential privacy attack for simplicity. However, it has been shown that other classes of privacy attacks (model stealing, model inversion etc) are also very much possible with the two ways of attacking mentioned and DP potentially can safeguard against a few other attacks besides MIA Rigaki and Garcia (2023).

Miró-Nicolau et al. (2024); Lyu et al. (2024), **Robustness** Alvarez-Melis and Jaakkola (2018); Mishra et al. (2021), **Localization** Zhang et al. (2018); Theiner et al. (2022); Kohlbrenner et al. (2020); Arias-Duart et al. (2022), **Complexity** Chalasani et al. (2020); Bhatt et al. (2020a); Nguyen and Martínez (2020), **Randomization** Adebayo et al. (2018); Sixt et al. (2020), are mostly accentuated in previous studies.

Unequivocally, **faithfulness** is the most crucial among all Miró-Nicolau et al. (2024); Lyu et al. (2024). **Faithfulness** is loosely defined as how well the explainer reflects the underlying reasoning of the model and has been extensively quantified in diverse ways Li et al. (2023); Hedström et al. (2023): **Sufficiency** (SF) Dasgupta et al. (2022), **Infidelity** (IF) Yeh et al. (2019), **Insertion/Detection AUC** (I/D-AUC) Petsiuk et al. (2018), **Pixel Flipping** (PF) Bach et al. (2015), **Iterative Removal of Features** (IROF) Rieger and Hansen (2020), **Ordered Perturbation** based metrics (OPs) Samek et al. (2016) are to mention a few. However, the evaluation metric(s) are not necessarily flawless; which we're going to discuss next.

3.3 Pitfalls of the Evaluation Metrics

Firstly, in the perturbation-based metrics such as PF, I/D-AUC, IROF, IF etc while applying operations such as flipping the pixels, inserting and/or deleting features, performing **meaningful perturbation** on the input space to generate synthetic inputs as a part of their evaluation process, do not crosscheck whether the generated input is out-of-distribution with respect to the trained model Hase et al. (2021); Chang et al. (2018). Secondly, metrics such as **OPs** are often excessively similar to the mechanics of the explainer itself. Instead of evaluating **faithfulness**, these methods primarily compute the similarity between the evaluation metric and explanation techniques, assuming the evaluation metric itself to be the ground truth Ju et al. (2021). Li et al. Li et al. (2023) has acknowledged the same in their benchmark \mathcal{M}^4 that LIME Ribeiro et al. (2016) and **OPs** are methodologically similar thus, the evaluation maybe skewed. Thirdly, previous studies have extensively shown that test-time input ablation is often prone not only to generating out-of-distribution (OOD) synthetic input Hase et al. (2021); Haug et al. (2021); Chang et al. (2018); Janzing et al. (2020) but also are *socially misaligned* Jacovi and Goldberg (2021). Thus, metrics for example I/D-AUC, IROF etc are suspected to be severely misleading. Quantitative metrics such as SF are also substantially constrained and do not provide a universal overview of **faithfulness**. Lastly, all these evaluations are based on naive assumptions (e.g.: erasure Jacovi and Goldberg (2020)), derived from a set of seemingly valid observations. Therefore, these quantitative metrics are not necessarily axiomatically valid. Even axiomatic necessary tests such as **Model Parameter Randomization test** Adebayo et al. (2018) happen to have a set of empirical confounders Yona and Greenfeld (2021); Kokhlikyan et al. (2021); Bora et al. (2024). To the best of our knowledge, there has not been any universally valid necessary and sufficient approach for faithfulness evaluation Lyu et al. (2024).

Furthermore, the lack of a unified faithfulness evaluation method and the absence of ground truth for explainers lead to the well-known disagreement problem Evans et al. (2022); Neely et al. (2021); Roy et al. (2022); Krishna et al. (2022). Even if explainers are **faithful**, their inherent mechanisms for calculating feature importance can lead to different explanations. For instance, Han et al. Han et al. (2022) demonstrated that while a subset of

commonly used XAI methods are all local function approximators, they employ different kernel and loss functions. Consequently, like **faithfulness**, other parameters for evaluating explainers are also contentious. For example, **adversarial robustness** (of the explainer) assumes that similar inputs with similar outputs should yield similar explanations Sinha et al. (2021); Ivankay et al. (2022). However, Ju et al. Ju et al. (2021) has empirically shown that the change in attribution scores may be because the model’s reasoning process has genuinely changed, rather than because the attribution method is unreliable. Moreover, this assumption is mainly valid when the model is *astute* Bhattacharjee and Chaudhuri (2020) and doesn’t necessarily apply to explainers that don’t perform local function approximation for feature importance estimation Han et al. (2022). In the subsequent section(s) we’ll try to figure out whether we can bypass these limitations for our study.

3.4 Aspiration for the Alternatives

Acknowledging these inherent limitations in current evaluation methods, we propose two key remarks:

1. **Remark 1.** Expert oversight should determine whether an explanation is *suitable* for high-stakes applications.
2. **Remark 2.** Explanations should align with local constraints and contexts, even when (so-called) *faithfulness* cannot be measured reliably.

To address the first requirement, in our use case we ensure that concerned physicians first receive X-ray images along with predictions and explanations. Results are only communicated to patients after the physician has completed a formal review and certified both the prediction and the explanation.

For the second remark, we are introducing the **localization assumption** (LA) and quantifying the same with a class of measures we collectively named the Privacy Invariance Score (PIS) for explanations.

4 Localization Assumption & Privacy Invariance Score

Right-to-Privacy (RTP) Thomson (1975) and Right-to-Explanation (RTE) Vredenburgh (2022) are two inalienable aspects of modern-day ML software. We have already mentioned that previous works have shown potential security breaches leveraging the explanation in section 3.1. So, RTE can hamper RTP but is the converse true? If yes, How can we quantify the same? We first propose the desideratum for explanations in this setting and then run extensive experiments to quantitatively *judge* the explainers.

4.1 Description of the setting

It is shown that adversaries can leverage *sensitive* information from explanations but due to post-processing of DP, any DP model will always output private explanation Dwork et al. (2014). We want to check the extent to which the explanations from a DP model can be used as a proxy for that of the non-private model here. Formally, for a non-private model \mathcal{M} , its private counterpart \mathcal{M}' ; consider a set of post-hoc explainers \mathcal{E} used for auditing

\mathcal{M} and \mathcal{M}' . For an input $x \in X$ (where X is the valid input space), each $\mathcal{I} \in \mathcal{E}$ produces explanations s and s' of x for $\mathcal{M}(x)$ and $\mathcal{M}'(x)$ respectively, Privacy Invariance Score (**PIS**) over a given tuple $(\mathcal{M}, \mathcal{M}', x, \mathcal{I})$ is defined as follows.

Definition 1. Privacy Invariance Score (**PIS**): Given a tuple $(\mathcal{M}, \mathcal{M}', x, \mathcal{I})$ given $\mathcal{M}(x) = \mathcal{M}'(x)$, PIS is defined as $sim(s, s')$. Where $sim(\cdot, \cdot)$ is a *similarity* metric, $s = \mathcal{I}(\mathcal{M}, x)$, and $s' = \mathcal{I}(\mathcal{M}', x)$.

4.2 Localization Assumption

As discussed earlier, different works evaluated explainers in various ways. These ad-hoc norms are often unique to each paper and inconsistent Jacovi and Goldberg (2020). However, practitioners have proposed some necessary axiomatic desiderata Lyu et al. (2024) such as the well-established **Implementation Invariance (II)** criterion proposed by Sundararajan et al. Sundararajan et al. (2017).

According to **II** if \mathcal{I} is *faithful* and $\mathcal{M}(x) = \mathcal{M}'(x) \forall x \in X$, i.e. $\mathcal{M}, \mathcal{M}'$ are *functionally equivalent* (FE) then $s = s' \forall x$. Commonly used explainers like **Integrated Gradient** Sundararajan et al. (2017), **SmoothGrad** Smilkov et al. (2017), **DeepLift** Li et al. (2021), **layerwise relevance propagation (LRP)** Montavon et al. (2019) etc had been extensively accessed based on **II** Sundararajan et al. (2017).

Following the line of prior explainability research, Jacovi et al. Jacovi and Goldberg (2020) formally proposed **The Model Assumption (MA)**:

“Two models will make the same predictions if and only if they use the same reasoning process.”

Nevertheless, in our setting, as the accuracy of \mathcal{M}' is generally less Ji et al. (2014), and we cannot say \mathcal{M} and \mathcal{M}' are FE Sundararajan et al. (2017). Furthermore, as X in practice can be arbitrarily large (theoretically could be countably infinite), quantifying whether an explainer (\mathcal{I}) is *sufficiently* trustworthy or not is often impractical. Also, finding a counterexample that violates the condition implying \mathcal{I} is not faithful is computationally expensive. Hence, we modify **MA** and propose the **localization assumption** for evaluating the explainers' quality in our setting.

First of all, in both the **II** and **MA** we do not advocate comparing any arbitrary models trained on the same data, having the same X to compare. For example, for a finite X , a trained neural network and a decision tree could have the same prediction $\forall x \in X$. That doesn't mean their *reasoning* is similar as the algorithms themselves are different. However, the private model \mathcal{M}' , in our setting, has identical architecture to that of \mathcal{M} . The fundamental goal of differential privacy is assumed to be masking individual contributions of the training set rather than completely changing its overall reasoning. However, as noise is induced in the gradient during the training, the parameters are expected not to remain entirely the same in the private model. Therefore, we assume that their reasoning should primarily be *similar*, if not the *same*. Formally, our adapted version of the **MA** is:

Assumption 1 The Localization Assumption (LA). *For a given tuple $(\mathcal{M}, \mathcal{M}', x, \mathcal{I})$ having $\mathcal{M}(x) = \mathcal{M}'(x)$, $sim(s, s') \geq \theta$. Where θ is a predefined similarity threshold.*³

3. It is worth nothing that **LA** and **Localization** discussed in 3.2 are different.

In this context, since we are using a proxy model (in our case, a DP model) as a substitute for the original model (the non-private model), we argue that beyond satisfying LA, the system must also meet two additional requirements:

1. **Performance comparability** (*Perf Comp.*): The proxy model should achieve comparable performance metrics to the original model. For this study, we focused on accuracy (acc) since in our test set, we put equal weightage on all classes and there is no class imbalance (further details are provided in Section 6). Specifically, we report $Acc_{\mathcal{M}'/\mathcal{M}} = \frac{acc. \text{ of } \mathcal{M}'}{acc. \text{ of } \mathcal{M}}$ for our experiments.
2. **Alignment with the original model** (*Alignment*): The proxy model must closely align with the original model in its predictions. In our study, we measure the same with the agreement on the “hard predictions” obtained from \mathcal{M} and \mathcal{M}' over the test set. (Dis)agreement has been extensively used in previous studies due to its simplicity and interpretability Shamir and Coviello (2020); Skalak et al. (1996); Liu et al. (2022); Milani Fard et al. (2016).

These two requirements are critical for ensuring the effectiveness of the proxy model. *Perf Comp.* is necessary because a significant drop in the proxy model’s performance would undermine its utility as a stand-in for the original model, especially in high-stakes applications. *Alignment* is equally important because, without sufficient agreement on predictions, the proxy model will fail to replicate the original model’s decision-making patterns, making it ineffective as a proxy. We refer to a proxy model that meets both these requirements as *functionally comparable* w.r.t. the original model.

Next, we investigate how we can measure the ‘similarity’ described in the **Localization Assumption**.

4.3 The Notion of Similarity

As previously discussed in PIS, we aim to measure the similarity between pair of explanations ; it is essential to account for two key factors here: the context of comparison and human understanding of that comparison. In this framework, given $(\mathcal{M}, \mathcal{M}', x, \mathcal{I})$ and $\mathcal{M}(x) = \mathcal{M}'(x)$, we seek to investigate two primary aspects:

- To what extent do s and s' agree?
- Wherever they agree, what is the degree of that agreement?

Firstly, explanations generally contain both positive and negative attributions⁴. For a classification, the positive attributions contribute in the favor of the classification while the negative ones don’t. Keeping this in mind, in order to address the first question, we start by calculating the number of places in both explanations where they yield different types of attribution scores; we denote this as the disagreement score (DS, measured in %). As both s and s' comprise attribution scores (per pixel or per element) that either positively contribute to the classification or do not, DS serves as a (crude) measure for assessing how

4. But a few explainers such as **Saliency** only outputs positive attributions; **Saliency** in particular, outputs the absolute value of the attributions.

much the reasoning of the models, as indicated by \mathcal{I} , diverges at the pixel or element level. Consequently, in a complementary manner, we focus on identifying the set of pixels selected by both models for classification. For instance, if the disagreement score is 0, it indicates that both models select the exact same set of positive and negative pixels (or elements) for classification. Conversely, a certain percentage of disagreement implies that \mathcal{I} reveals differences of reasoning in how \mathcal{M} and \mathcal{M}' interpret pixel(s) for the same classification task.

From a human evaluation perspective though, analysis on DS is context-sensitive. While evaluating DS may not be crucial in all applications, it becomes critically important in high-stakes domains, such as biomedical software, where discrepancies could lead to significant confusion. In these contexts, both position and attribution of information are vital for accurate treatment decisions. To address this, our system evaluates disagreement at an atomic level, ensuring precision and thoroughly scrutinizing the explainer when a specific threshold of disagreement is identified for an image. In our study, we set the DS threshold 15%. We employ DS primarily as a sanity check in our experiment for the comparability of model explanations.

To tackle the second question, after measuring DS and eliminating the ones not adhering the threshold, we assess how the attribution assignments correlate with each other. However, the correlation at pixel-level attributions is inherently a crude estimate. Given that each input image includes over 50,000 pixels, computing correlation directly is computationally demanding. Thus, we employ a two-step approach here.

Firstly, we segregate the positive attributions from the negative ones. This distinction is crucial because positive pixels contribute positively to the classification, while negative attribution scores may indicate a range of scenarios: a pixel could primarily (or completely) contribute to other classes, contribute negatively to the output class, or any combination of these two Ancona et al. (2017); Samek et al. (2017). This is why we solely focus on the pairwise positive pixels from both explanations and compute their rank correlation with the nonparametric Kendall Tau⁵. We empirically set a (crude) baseline (in a context aware fashion) of 0.5 (50% positively correlated) for the comparison. Our approach is easily implementable with commonly used libraries such as `tf-explain`⁶ and `Captum`⁷.

4.4 Other notions for Similarity

Can cosine similarity be an alternative? : Mostly No, as in such high dimensions the large random vectors are almost always *almost orthogonal* if they are not (condensely) clustered Mohammadi and Petridis (2022); Wyner (1967). Moreover, unlike the correlation and disagreement cosine is not that much nuanced as this doesn't compare the Condorcet pairs but imposes a vague sense of how much the vectors are 'aligned' defined over their inner product space in such high dimension which doesn't go with our objective.

5. A natural question might arise: What if all the pixels have negative attributions? As we are taking the explanation against the "hard prediction", if an explanation is not having any pixel with positive attributions yet it predicted the selected class; we'd argue its **faithfulness**. As a negative attribution across all pixels would suggest that the model made its prediction without relying on any relevant pixel/element from the input image. Moreover, throughout our experiments we never encountered such instance and positive attributed pixels were never < 60%

6. <https://tf-explain.readthedocs.io/en/latest/>

7. <https://captum.ai/>

Can L_P norms be a better metric? No, we need to normalize before comparing the vectors, which kills one degree of freedom, which is not the case with correlation.

5 Experimental Setup

5.1 Description of the Dataset

Our dataset comprises 2,000 Pneumonia cases sourced from the Chest X-ray dataset by Sharma et al. Sharma (2020), and 2,000 TB cases randomly sampled from the NIAID TB Portal Program dataset National Institute of Allergy and Infectious Diseases (n.d.). To create the ‘Normal’ subset, we include an equal split of 1,000 unaffected Pneumonia samples from the uneffected class in the aforsaid Chest X-ray dataset Sharma (2020) and 1,000 unaffected TB samples from Rahman et al. Rahman et al. (2020), totaling 2,000 normal cases. For evaluation, the test set contains 200 images for each class.

This paper, unlike prior studies, is not focused on the empirical studies of private models in healthcare Zerka et al. (2020); Naresh et al. (2023); Khalid et al. (2023). Instead, we concentrate on the applicability of commonly used explainers in a privacy preserving environment. Our aim is to investigate whether RTE and RTP can be achieved simultaneously. As a result, rather than a large dataset where extensive experimentation with DP under a closely controlled environment is computationally expensive and cumbersome Subramani et al. (2021), we focus on first making a dataset of an appropriate size where we have considered the commonly available and utilized disease class from the previous studies: Pneumonia, Tuberculosis (TB). However, after our primary experiment, we devise the same setup for another benchmark dataset: CIFAR-10 but we arrived at similar conclusion. Details can be found in Appendix B.

5.2 Choosing the privacy budget *aka* ‘ ϵ ’

The determination of privacy requirements and expectations is a critical aspect of our experimental setup. However, selecting ϵ comes with a notable dichotomy:

The theoretical school advocates for stringent privacy guarantees, proposing $\epsilon \leq 1$. This conservative approach provides robust worst-case guarantees against inference attacks. For instance, in the case of, $\epsilon \leq 0.1$ ensures that no membership inference attack (MIA) can outperform random guessing by more than a marginal 2.5% (i.e., 52.5% success rate).

Conversely, industrial implementations often employ substantially larger values, typically $\epsilon > 7$. According to the theoretical school such choices, while pragmatic, significantly increase vulnerability. With such choices of ϵ , system becomes severely vulnerable with the worst case MIA attack succeeding rate exceeding 99%.

This stark contrast stems from divergent underlying assumptions Lowy et al. (2024):

- The theoretical model assumes an adversary with near-complete knowledge of the training set, lacking information on only a single data point.
- It also presupposes uniform privacy guarantees across all data points.

Very recently, Lowy et al. (2024) has shown why often these assumptions are not relevant in practical and industrial settings and DP with large ϵ (even $\epsilon \geq 7$) can sufficiently defend

against practical and implementable MIAs. Furthermore, in reality, training data is typically either fully public (subject to regulatory compliance) or entirely private. Particularly in several high-stakes domain, data breaches and unauthorized access to sensitive information (e.g., healthcare records) often result in comprehensive system restrictions, as exemplified by Italy’s 2023 temporary ban on ChatGPT due to privacy concerns McCallum (2023).

Nevertheless, this study is *not* about how to choose ‘ ϵ ’ for the biomedical software(s). Moreover, such questions are open-ended and as far as healthcare is concerned, it is more on the side of the authoritative bodies on how they impose the guidelines rather than individual stakeholders. In this study, we follow the guidelines proposed by Google where they introduced a three-tier system Ponomareva et al. (2023).

- Tier 1: $\epsilon \leq 1$
- Tier 2: $\epsilon \leq 10$
- Tier 3: $\epsilon > 10$

Tier 1 matches the theoretical view but loses too much utility in real-world settings. Tier 2 is advocated by Google as it adheres to practical constraints and yields reasonable privacy-utility trade-off. Lastly, tier 3 is avoided in this study as it makes the system excessively vulnerable.

Our primary investigation examines six discrete ϵ values: 0.4, 0.7, 1, 4, 7, and 10. This range enables a comprehensive analysis of the privacy-utility trade-off spanning across tier 1 and tier 2.

5.3 Description of the Explainers

We primarily selected gradient-based explainers which are predominantly used in computer vision tasks Buhrmester et al. (2021) — specifically, **Saliency**, **SmoothGrad**, **Integrated Gradients**, **Grad-Shap** and, **Grad-CAM**. These gradient-based explainers rely on the sensitivity the model shows to the features subject to the output it obtains. In other words, these explainers leverage the gradient of the output (or any selected class of interest) w.r.t. the input features⁸. For example, **Saliency** computes the partial derivatives of the output with respect to the input given, **Integrated Gradients** computes the average gradient while the input varies along a linear path from a baseline. **SmoothGrad** involves adding noise to the input image and generating multiple saliency maps, each corresponding to a slightly different noisy version of the input image; the saliency maps are then averaged to produce a ‘smoothed’ saliency map. **Grad-CAM** also involves taking gradients of the target output with respect to the given layer. From perturbation-based explainers, we included only **SHAP** Lundberg and Lee (2017), specifically **Grad-Shap**, as core perturbation methods are less widely adopted for computer vision. **Grad-Shap** can be viewed as an approximation of **Integrated Gradients** by computing the expectations of gradients for different baselines⁹. Other perturbation-based methods like **LIME** Ribeiro et al. (2016) assign weights to super-pixels rather than individual pixels as a result, we cannot compare the same with other methods we chose which output

8. it can either directly be the element(s) of the given input or the intermediate ones coming from a layer inside the model.

9. Captum

per-pixel or per-element attribution values, **Occlusion** can lead to OOD artifacts and is not widely used Chang et al. (2018). Additionally, some other explainers such as **DeepLIFT**, **LRP** disregard even basic faithfulness tests Sundararajan et al. (2017).

5.4 Description of the Networks

Disease detection using chest X-ray is a well-regarded case study. In previous works Al-qaness et al. (2024), the choice of CNNs is significantly prominent and in this work also we have chosen the famous CNNs that had been used in previous research. Particularly, We selected ResNet-34 He et al. (2016), EfficientNet-v2¹⁰ Tan and Le (2021), and DenseNet-121 Huang et al. (2017) for our analysis due to their competitive performance. Importantly, we ensured that the DP counterparts of these models were *functionally comparable* across a wide range of values for ϵ , to the best of our ability. However, previous studies have shown that DP doesn't make the model learn all classes in a comparable fashion Suriyakumar et al. (2021); Fioretto et al. (2022) as a result, we report the accuracy (acc) as a measure of *Perf Comp.* and agreement on "hard prediction" to measure *Alignment* on a class-wise basis, allowing for a more nuanced comparison.

We train the non-private and private models fixing all the hyperparameters except for the number of epochs, as private models need more computation to learn due to the heavy regularization DP introduces in the training Ponomareva et al. (2023). However, to make a fair comparison we have fixed the number of all hyperparameters in all the private models with different ϵ ¹¹.

However, while training we discovered an issue in the vanilla architecture of the aforementioned networks: they utilize batch normalization (**BatchNorm**). Nevertheless, **BatchNorm** normalizes a sample based on the statistics of the batch it is in. This means the same sample can get different normalized values depending on the other samples in the batch. For differential privacy, each sample's privacy needs to be independently preserved. Since **BatchNorm** depends on other samples, it violates this principle and leaks information about other samples. Yousefpour et al. Yousefpour et al. (2022) advises replacing **BatchNorm** layers with privacy-friendly options like Group Normalization, Layer Normalization, Instance Normalization etc. From the engineering perspective, we have to select one such replacement that scales with sufficiently large datasets without hampering the privacy bounds. Based on previous empirical evidence Subramani et al. (2021), we replace the **BatchNorm** layers with **GroupNorm** layers in all non-private models along with their private counterparts, as **GroupNorm** does not alter the base architecture drastically, scales well and adheres to the privacy principle strictly. We employ the DP-SGD algorithm for the private training Abadi et al. (2016). The non-private models' accuracies are reported in Table 1 and in Figure 1, 2, 3 for private counterparts.

10. For this study, we used the 'small' version from the EfficientNet-v2 family, referred to throughout the paper as EfficientNet-v2.
 11. We set the no. of epochs as 50 for all private models; it yielded competitive accuracy across model types. However, within 13 – 16 epochs, all non-private models achieved accuracy $> 95\%$.

	TB Acc. (%)	Pneumonia Acc. (%)	Normal Acc. (%)	Overall Acc. (%)
DenseNet	95.0	97.5	97.2	96.55
EfficientNet	93.5	96.2	96.0	95.57
ResNet	93.2	96.0	96.3	95.51

Table 1: Acc. Table for models.

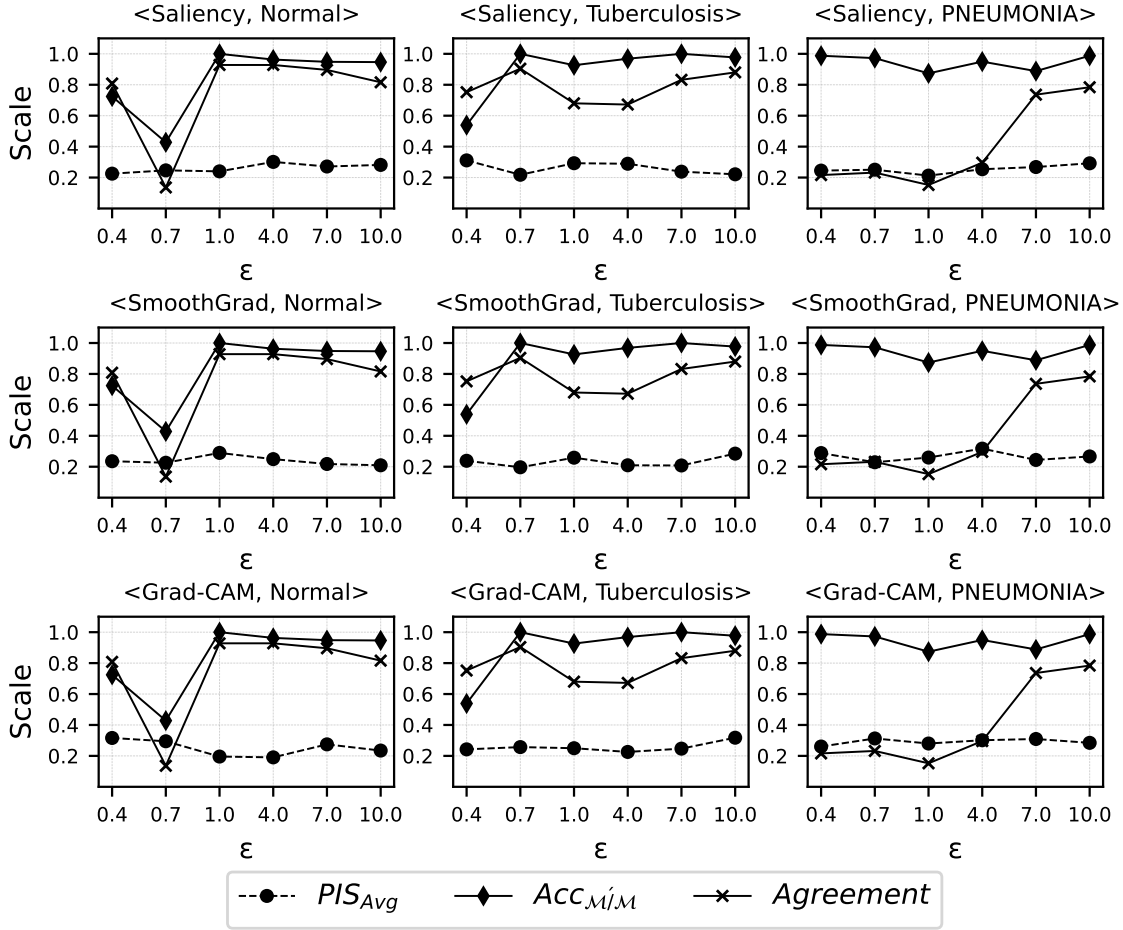


Figure 1: Performance of the post-hoc explainers (DenseNet-121)

6 Key Observation

In this section, we present our experimental results to find out whether the post-hoc explainers agree with the **Localization Assumption** (LA), defined in Section 4.2. **Integrated Gradients** and **Grad-Shap** showed more than 45% DS everywhere which directly violates our DS threshold of 15%. As we consider DS a sanity check for LA, and these two explainers fail this test, we exclude them from further discussions. Across models, around 30 – 40% **Grad-Cam** explanations of test samples violated the DS threshold, we have considered the

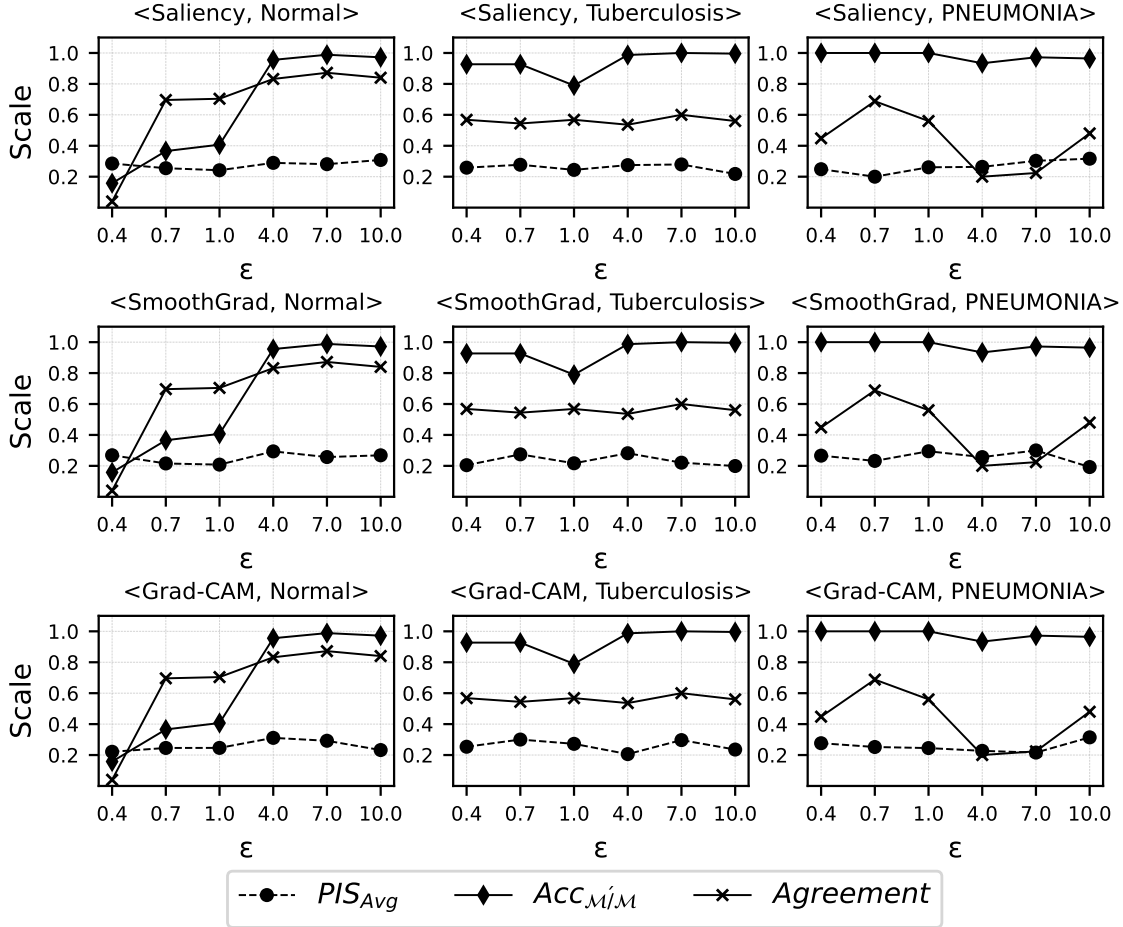


Figure 2: Performance of the post-hoc explainers (ResNet-34)

rest of the samples to calculate PIS. Almost all test samples passed the DS test across models for **Saliency** and **SmoothGrad**.

We report our findings for the three networks: DenseNet-121, ResNet-34 and EfficientNet-v2 in Figure 1, 2 and 3 respectively. For each of these networks, we report class-wise results against each of the three explainers which pass the DS test. Against each ϵ , we report average of the PIS values over the test set (PIS_{Avg}), $Acc_{\mathcal{M}'/\mathcal{M}}$, and agreement on the “hard predictions” obtained from \mathcal{M} and \mathcal{M}' over the test set (*Agreement*). PIS_{Avg} gives the extent to which an explainer agrees with the LA in a particular setup; $Acc_{\mathcal{M}'/\mathcal{M}}$ quantifies the *Perf Comp.* requirement, and *Agreement* quantifies the *Alignment* requirement for the private model to be *functionally comparable* w.r.t. the original model, defined in Section 4.2. We observe all of the explainers across ϵ , classes, and models are performing poorly in terms of PIS_{Avg} ¹². In fact, the PIS_{Avg} never crosses 0.32; such a low PIS_{Avg} indicates that none of the explainers agree with the LA. Almost all cases except for the Normal class against low

12. One may argue that what if we measure similarity without segregating attributes? This although disregards our philosophy on similarly measure still we did and to be precise, never found $PIS_{Avg} > 0.16$.

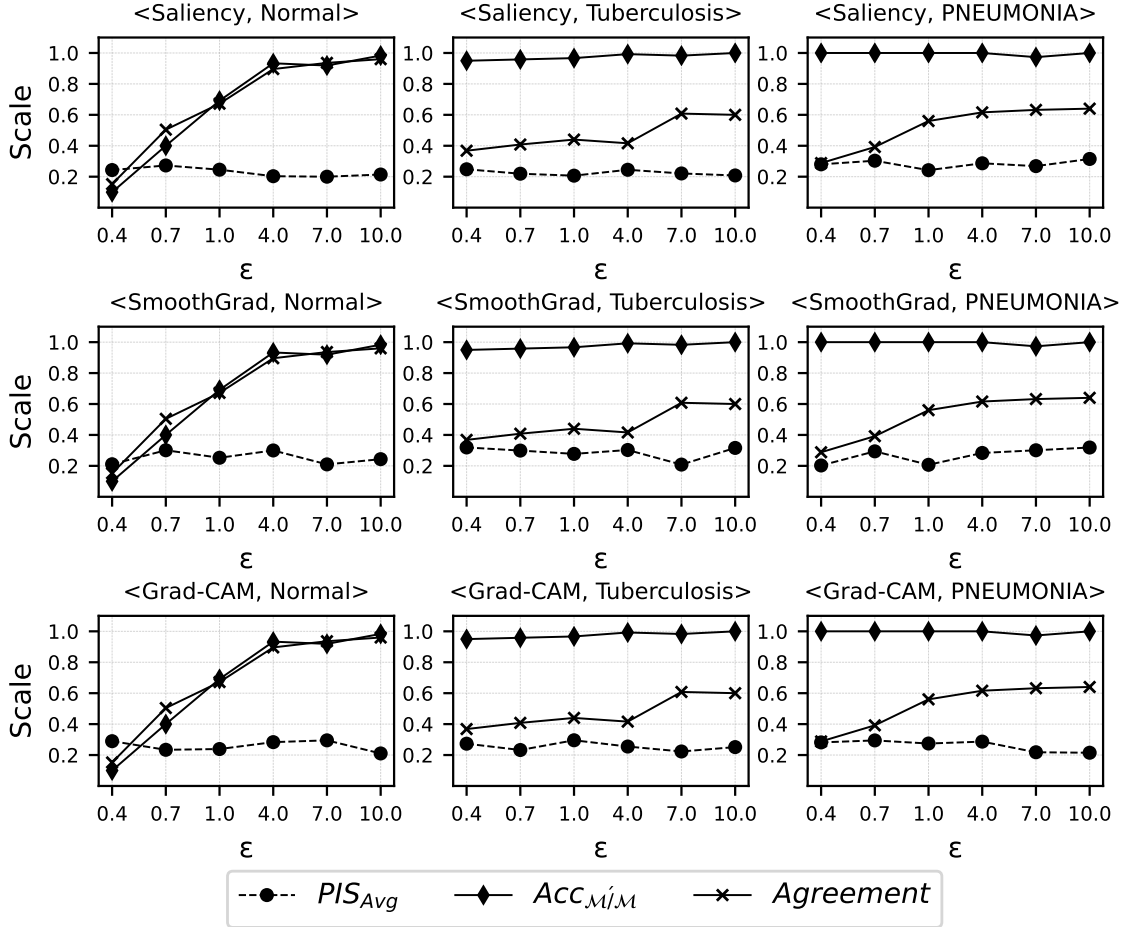


Figure 3: Performance of the post-hoc explainers (EfficientNet-v2)

ϵ values, $Acc_{M'/M} \approx 1$, which indicates that almost all private models achieved near equal accuracy as of their base counterparts. Nearly 70% of cases achieved $Agreement > 0.50$. There is no apparent relation or trend the PIS_{Avg} follows with $Acc_{M'/M}$ and $Agreement$. All in all, the explanation quality is consistently poor no matter what happens to the other parameters. Empirically, it is clear that all gradient-based explainers disregard LA, but why is it so? We'll try to find out in the next section.

7 Why Explainers Performed so *Poorly*?

As noted in the previous section, the explanations from private and non-private models are largely uncorrelated. Private models are trained using DP-SGD, which involves gradient clipping and adding calibrated noise during backpropagation to achieve DP. To understand the divergent behavior of explainers between these models, we first analyze how DP training alters model parameters. We conduct a comparative study on the (layerwise) representations learned by both private and non-private models, followed by a rigorous investigation into

the (local) sensitivity of these representations. While the former reveals how DP training modifies the parameter space, the latter explains how these modifications influence the model’s reaction to inputs, ultimately affecting explainer behavior. To the best of our knowledge, this is the first study to comprehensively examine the representations learned by DP models and compare them to non-private models. Moreover, the layer-wise sensitivity analysis has not been previously explored for any model, including DP models. We include the implementation details in Appendix C and will publicly share the weights and codes upon publication.

In its forward pass, a neural network hierarchically transforms the given input into increasingly abstract (and complex) representations. A Representation (also referred to as a feature representation or simply {intermediate} feature) is the set of activations stored layerwise in the network during the forward pass for a given input. We begin our investigation by examining how these representations differ in the private and non-private models, as this reveals how these two different models process and transform the input data across layers. Understanding the alignment of these representations is critical for analyzing how DP training has altered the model’s parameters and how these changes influence the model’s overall reasoning.

However, since the training processes for DP model is fundamentally different and designed to achieve distinct goals, we first conduct a formal assessment to determine whether any statistical dependence exists between their layerwise representations. This step ensures that the representations are comparable before further analysis. We denote the representation at layer l as σ_l .

Statistical tests for activations are often non-trivial and subject to a few constraints such as invariance to permutation of the neurons, orthogonal transformation (Klabunde et al., 2024) etc. Consequently, we use the Hilbert-Schmidt Independence Criterion (HSIC) (Gretton et al., 2007) which operates over a Reproducing Kernel Hilbert Space (RKHS) and can detect dependencies across complex, high-dimensional variables while respecting the aforesaid constraints. We employ the HSIC unconditional independence test using the two-parameter γ approximation scheme with a p-value cut-off of 0.05 (Gretton et al., 2012).

From our findings, we were **able to reject** the null hypothesis \mathcal{H}_0 for almost all layers¹³. In other words, across models layerwise representations are **not** independent, for all ϵ . Since the representations are sufficiently comparable, we’ll now compute their similarity layerwise. However, before a full-fledged comparison, we present a short note on representational similarity (RS).

7.0.1 ON REPRESENTATIONAL SIMILARITY

Representational similarity measures compare neural networks by computing similarity between activations of a fixed set of inputs (in our case, test set) at a given pair of layers. There’s been an extensive line of work on this domain however, each of them can be categorized depending on the notion of *similarity* it regards. Each similarity measure follows a set of assumptions. In our paper, we have considered the most regarded set of assumptions and its corresponding similarity measure, namely Centered Kernel Alignment (CKA) (Kornblith et al., 2019; Gretton et al., 2007). CKA is built upon HSIC and bounded

13. For example, across models we never crossed 7 – 10% of the layers for any ϵ where we accept \mathcal{H}_0

within the (closed) interval of $[0, 1]$. However, there are a few (discovered) shortcomings of CKA, as discussed below.

The wildly used CKA with the linear kernel, is equivalent to the RV coefficient and it is already shown that the same seldom yields values close to 1 due to one of its inherent shortcomings: although the coefficient is inherently constrained to values between 0 and 1, it *rarely* reaches values near 1 because the denominator is typically much larger relative to its theoretical maximum value (Puccetti, 2022). Also, the lesser adapted RBF-CKA is highly sensitive to the kernel width and ineffective for small values (Davari et al., 2022).

Furthermore, very recently Cui et al. (Cui et al., 2022) have discovered that the inter-example (dis)similarity in the representation space works as a confounder. In their words, “*This leads to spuriously high CKAs even between two random neural networks, and counter-intuitive conclusions when comparing CKAs on sets of models trained on different domains ...*”. They fixed this problem by regressing out the confounder from the similarity matrices of two representations. Our analysis uses this *deconfounded* version of CKA (dCKA). For HSIC, we used both linear and non-linear (RBF) kernels but obtained similar results.

In our approach, since both the non-private and private models share the same architecture, we perform a layer-wise comparison between the corresponding layers of the non-private model and its private counterpart(s). However, as the models under consideration are excessively large, reporting Representational Similarity (RS) for each activation layer individually can become overwhelming due to the sheer volume of data. Instead, depending on the number of layers, we grouped the activation layers into 15/17 clusters¹⁴ and reported the median RS for each cluster, as shown in Figures 4, 5, and 6. From our findings, it is evident that any pair of models learn somewhat similar representations. In the initial layers, they learn almost identical representations, but as we progress through the layers, the similarity deteriorates. Interestingly, the last few layers in all model pairs exhibit significant dissimilarity compared to the first few.

All in all, the private models don’t perceive the data in a strongly correlated manner w.r.t their non-private counterparts. However, we argue that this is not the only reason for the explanations to be altered, as explanations are based on the *sensitivity* of the features subject to a class of interest the model shows. In the second phase of our investigation, we shall look into how much, for an obtained output, the model is *sensitive* to all the layerwise representations it obtained in the forward pass.

7.1 Do the models show *similar* sensitivity?

In this section, we investigate how sensitive the model’s output is to the layerwise representations generated during the forward pass. Formally, for a given layer l and a class of interest (here, “hard prediction”) Θ , we compute the gradient: $\nabla_{\sigma_l} \Theta$. This gradient is particularly important for two reasons: first, it quantifies the influence of an infinitesimal perturbation in the representations at layer l on the final output. Second, as previously discussed in section 5.3, gradient-based explainers also leverage $\nabla_{\sigma_l} \Theta$ to generate explanations¹⁵. Thus,

14. For ResNet-34 and EfficientNet-V2, we considered all 17 ReLU and 102 SiLU layers respectively, constituting 17 clusters (17|102). For DenseNet-121, we considered all 120 ReLU layers, constituting 15 clusters (15|120).

15. Typically, l refers to the input layer, except for Grad-CAM.

explanations, in essence, can be unanimously viewed as the output of a class of *mechanisms* applied to $\nabla_{\sigma_l} \Theta$, subject to specific input(s), layers and/or baselines (wherever required).

This is why the comparability of explanations across models depends on whether $\nabla_{\sigma_l} \Theta$ obtained layerwise are comparable between private and non-private models. Moreover, as the level of abstraction in representations varies across layers, we examined $\nabla_{\sigma_l} \Theta$ at all activation layers to understand the full spectrum of sensitivity across the models.

However, unlike representations, working with $\nabla_{\sigma_l} \Theta$ presents a few more challenges. First, since it directly depends on the model’s final output, we need to ensure that both models predict the same class for the input instance in order to make the gradients comparable. If the models predict different classes, the gradients will reflect sensitivities toward those different outputs, making direct comparisons inappropriate. To address this, we could restrict our analysis to the subset of the test set where both models make identical predictions. However, this approach has a distinct problem: RS is calculated over the entire test set, whereas $\nabla_{\sigma_l} \Theta$ would be evaluated over this reduced subset. This mismatch in the sample space (test set) immediately invalidates the direct application of *any* quantitative similarity measures. Conversely, if we use the reduced dataset for evaluating RS, we will not be able to capture the *true* similarity between layers. Additionally, unlike RS, we lack well-established assumptions for defining similarity in the case of $\nabla_{\sigma_l} \Theta$. These inherent challenges make it hard to establish a one-to-one correspondence between the similarity of layerwise representations and the similarity of their corresponding sensitivity($\nabla_{\sigma_l} \Theta$).

Due to these inherent challenges, we only conduct hypothesis testing using HSIC, as previously mentioned, to check whether the sensitivity of representations is statistically (in)dependent, where the corresponding outputs match¹⁶. Here also, we employed both linear and non-linear (RBF) kernels but obtained similar results.

From our findings, we were **unable to reject** the null hypothesis \mathcal{H}_0 for across almost all layers¹⁷. In other words, unlike representations, the *sensitivity* of representations is independent across models. Regarding **Grad-CAM**, we typically use the last layer to generate the CAM. Our experiment showed that the gradients of these layers exhibit independence, meaning the CAMs produced by different models will not be comparable. Similarly, other explainers relying on $\nabla_{\sigma_l} \Theta$ cannot produce aligned and substantially comparable explanations, as representations across levels along with the last layer show **independent** sensitivity between non-private and their private counterparts¹⁸.

⦿ Overall, neither the DP models extract the features the way a non-private model does, nor they can exhibit the sensitivity over the features in a similar fashion. $\nabla_{\sigma_l} \Theta$ can be viewed as how Θ changes for a *infinitesimally* small perturbation around σ_l . We have observed σ_l are mildly similar across layers for non-private and private models; however, ‘ ∇ ’ operator being a crude first-order approximation only addresses the immediate, linear

16. Essentially, this is the dataset considered for PIS.

17. In no model did we reject \mathcal{H}_0 for more than 3-7% of the layers across ϵ . Notably, for DenseNet-121, all layers were found to be independent

18. A natural question arises: could an explainer, despite of consistently incomparable sets of $\nabla_{\sigma_l} \Theta$, produce similar explanations? Based on our experiments, we did not identify any commonly used explainer that exhibited this property for the models selected. Furthermore, we argue the **faithfulness** of such explainers, if they exist, would be questionable. Conversely, assessing the quality of explanations when (local) sensitivity is consistently comparable across *any* pair of models falls outside the scope of this paper.

response of the output w.r.t perturbations around σ_l which, in our case, is **independent** to that of non-private model(s). In other words, the *different* set of parameters obtained with DP training is **sufficient** for the non-private model to show divergent sensitivity across layers which, in turn, makes the explanations incomparable. DP training was primarily meant to resist MIA w.r.t. the training data but the training goes much beyond the scope, and drastically alters the overall reasoning dynamics of a model. Which, as demonstrated, makes the popular post-hoc methods nonfunctional.

$\epsilon = 10$	0.97	0.88	0.86	0.82	0.66	0.63	0.64	0.64	0.64	0.65	0.64	0.64	0.64	0.66	0.66	0.66	
$\epsilon = 7$	0.98	0.91	0.90	0.82	0.60	0.55	0.55	0.57	0.59	0.59	0.59	0.58	0.57	0.58	0.58	0.61	
$\epsilon = 4$	0.97	0.91	0.91	0.82	0.57	0.51	0.48	0.49	0.49	0.49	0.47	0.46	0.44	0.43	0.42	0.41	0.42
$\epsilon = 1$	0.96	0.88	0.88	0.83	0.65	0.61	0.60	0.59	0.59	0.61	0.62	0.62	0.62	0.61	0.62	0.60	0.64
$\epsilon = 0.7$	0.98	0.85	0.85	0.80	0.65	0.60	0.59	0.62	0.62	0.63	0.63	0.64	0.63	0.62	0.63	0.60	0.61
$\epsilon = 0.4$	0.97	0.89	0.89	0.82	0.62	0.59	0.57	0.58	0.58	0.60	0.62	0.63	0.64	0.64	0.67	0.64	0.63

Figure 4: dCKA heatmaps for ResNet-34

$\epsilon = 10$	0.94	0.87	0.83	0.75	0.76	0.72	0.69	0.71	0.70	0.69	0.71	0.71	0.71	0.71	0.71	0.71
$\epsilon = 7$	0.93	0.84	0.82	0.75	0.73	0.67	0.67	0.66	0.64	0.66	0.67	0.59	0.58	0.57	0.58	0.58
$\epsilon = 4$	0.91	0.84	0.81	0.75	0.76	0.71	0.68	0.71	0.67	0.71	0.73	0.73	0.70	0.70	0.69	0.69
$\epsilon = 1$	0.93	0.85	0.82	0.75	0.74	0.69	0.66	0.66	0.64	0.67	0.67	0.61	0.61	0.62	0.62	0.62
$\epsilon = 0.7$	0.92	0.87	0.82	0.74	0.74	0.66	0.66	0.67	0.62	0.66	0.66	0.63	0.61	0.60	0.59	0.59
$\epsilon = 0.4$	0.93	0.86	0.82	0.73	0.72	0.67	0.66	0.66	0.61	0.65	0.66	0.65	0.63	0.62	0.61	0.61

Figure 5: dCKA heatmaps for DenseNet-121

$\epsilon = 10$	0.94	0.80	0.48	0.49	0.48	0.49	0.49	0.50	0.50	0.51	0.49	0.52	0.47	0.44	0.43	0.44	
$\epsilon = 7$	0.93	0.75	0.52	0.51	0.47	0.45	0.46	0.46	0.47	0.45	0.45	0.41	0.40	0.37	0.36	0.37	0.39
$\epsilon = 4$	0.92	0.73	0.51	0.51	0.49	0.50	0.51	0.51	0.49	0.42	0.42	0.38	0.36	0.34	0.32	0.31	0.39
$\epsilon = 1$	0.92	0.71	0.52	0.53	0.53	0.55	0.56	0.57	0.55	0.52	0.50	0.47	0.44	0.41	0.37	0.36	0.46
$\epsilon = 0.7$	0.91	0.72	0.55	0.50	0.51	0.51	0.52	0.52	0.53	0.51	0.47	0.46	0.42	0.40	0.38	0.43	0.47
$\epsilon = 0.4$	0.89	0.75	0.60	0.48	0.43	0.43	0.44	0.46	0.47	0.47	0.44	0.42	0.41	0.43	0.37	0.39	0.44

Figure 6: dCKA heatmaps for EfficientNet-V2

8 Is there any alternative way to have private explanations?

We now know that the DP models cannot accommodate widely used post-hoc explainers primarily due to their own behaviour. As a result, we cannot move forward with DP models to obtain private explanations. However, just for private explanations, we don't need that. We can achieve the same *locally* as well.

In this approach, rather than training the model with DP-SGD, we use the non-private model as usual and take their explanations. We add calibrated noise to the explanation to make it Local Differential Private (LDP)

- Formally, given a function $f : D \rightarrow \mathbb{R}^d$, the Laplace mechanism \mathcal{A} is defined as:

$$\mathcal{A}(D) = f(D) + \text{Lap}(0|t)^d$$

Where \mathcal{A} satisfies ϵ -differential privacy for $t = \frac{\Delta f}{\epsilon}$, and Δf is the sensitivity¹⁹ of f Dwork et al. (2014).

Here, Noise is directly applied to the heatmap obtained from the explainer. Following the guidelines by Fan (2018), for an image with c channels, each of which spans k possible pixel intensities, the sensitivity of the query is $(k-1)nc$, where n is the maximum number of pixels that can differ in two adjacent images. Given this query sensitivity, ϵ -differential privacy can be provided by independently applying the Laplace mechanism to each pixel in each channel, using a scaling parameter of $(k-1)nc/\epsilon$. However, such a large amount of noise, especially for smaller ϵ , would completely obfuscate the semantics of the image. To reduce the query sensitivity, the authors propose dividing the image into $b \times b$ grids of pixels, where each grid is averaged to create a uniform value. Treating each grid as a single unit to be obfuscated reduces the required scaling parameter to $(k-1)nc/b^2\epsilon$. Therefore, in the case of explanations (or likewise *any* heatmap with 1 channel), the query sensitivity is $255n/b^2$.

Any *valid* set of n and b chosen by the user ensures ϵ -differential privacy, but tuning these parameters offers a trade-off between privacy and utility. Therefore, this framework allows us to generate explanations that are both useful and private.

Here, a natural question arises: what constitutes a *good* value for n ? Previous works have tackle this problem empirically as this primarily depends on the use-case. We, therefore, empirically tested with a diverse set of (n, b) and communicated the results with the physicians of SRM University AP. We get the best response for the tuple $(16, 14)$, and the most competent explainers were **Grad-Shap** and **Integrated Gradients**. In our case, we get useful results $\epsilon = 4$ onwards. We selected the ResNet-34 for demonstrating our results and we have reported explanations from all four explainers in Appendix A.

8.1 What Could Be the Notion of PIS and LA Here?

After *LDP-fying* with $b \times b$ grids, we cannot compare explanations *pixel-to-pixel*. Here, our motivation is to compare how much *LDP-fying* degrades the *quality* of the explanation, to measure that we have to change the similarity measure accordingly. That is why here, unlike global DP, we do not measure DS or correlation but following the postulate of LA, we expect that the *most competent* explanation should be least *affected* and thus should be most *similar* and can be a close proxy to the actual explanation. For the notion of PIS, we measure the *similarity* of the newly made explanation image with Structural Similarity Index (SSIM) Wang et al. (2004). SSIM is suitable here because it captures perceptual similarities rather than exact pixel values, which is crucial for understanding qualitative degradation. While *pixel-by-pixel* comparison may not be sensitive to perceptual changes, SSIM evaluates structural components—luminance, contrast, and structure—that reflect images are *visually processed* (by the observer). In this context, SSIM effectively measures the similarity by capturing how much essential information is retained after privacy transformations, aligning

19. This sensitivity is different from the (local) sensitivity we discussed in section 7.

with our goal of assessing how closely the modified explanation approximates the original. The most robust explanation will remain minimally affected, thus showing the highest SSIM, making it a strong proxy for maintaining interpretability under privacy constraints.

However, in this setup, we face a challenge to work with **Grad-CAM**. It produces a region of interest (ROI) rather than a per-pixel attribute score which is substantially small (a grid of 7×7 or 8×8). Fixing the hyperparameters in the ROI to make it LDP, we found substantially challenging as even minor noise overwhelms the attributions due to the relatively small number of pixels in ROIs, as a result, we have to discard the same from further evaluations. For demonstrating purposes, we have chosen the ResNet-34 for our software and reported the mean SSIM value for each class and explanations in table 8.1. However, here in this setup, we do not put any presuppositions on the baseline unlike global DP and adopt ad-hoc strategy to set the threshold as long as the private explanations are approved by the concerned physician(s) as there is an inherent trade-off between explanations' *quality* and *privacy guarantee*.

Quality of the explanation (SSIM here) evaluates the perceptual similarity of two images by comparing structural and luminance components. However, introducing LDP noise degrades these structural details to protect individual pixel-level information, thereby reducing SSIM. Balancing the degree of noise to achieve a desired privacy level inevitably diminishes SSIM, as high privacy requires more noise, which more significantly impacts the structural fidelity of the image. Our set of hyperparameters craftfully strikes the balance and produces succinctly practitioner-approved private explanations. In our experiment, we roughly get PIS between $0.4 - 0.5$ for all explainers.

	Grad-SHAP	Integrated Gradient	Saliency	SmoothGrad
Tuberculosis	0.52	0.50	0.49	0.52
Pneumonia	0.53	0.51	0.43	0.49
Normal	0.56	0.54	0.49	0.53

In this setup, the model is non-private but the explanations are private, we name this setup as **Hybrid DP**. Our novel software is outlined using this setup in Figure 9.

○ To summarize:

	Drop in Accuracy	Private Model	Private Output	Private Explanation	Useful Explanation
Global DP	✓	✓	✓	✓	✗
Hybrid DP	✗	✗	✗	✓	✓

9 The Novel Software

Based on our extensive findings, we propose a comprehensive software architecture that ensures both privacy preservation and model explainability. The system is designed with a scrutiny check and privacy-preserving components, orchestrated to work seamlessly while maintaining both RTP and RTE guarantees.

System Overview and Security Measures: At the entry point, all incoming images pass through an autoencoder (AE) that acts as the first line of security Neloy and Turgeon

(2024); Berahmand et al. (2024). We get 94.7% mean accuracy over anomalous inputs²⁰ at a reconstruction loss threshold (κ) of 0.04. This AE serves dual purposes: (i) it validates the authenticity of inputs by detecting anomalous patterns that might indicate adversarial attacks or corrupted data, and (ii) it ensures that only legitimate medical images enter the system’s processing pipeline. Images that deviate from κ are rejected, preventing potential security vulnerabilities.

Core Processing Pipeline: The validated images then enter the main processing pipeline, where our non-private model resides at the center of the system. This model is secured behind an API interface. It generates the prediction for given images which, over an encrypted channel, is received by the concerned physician(s). Note to mention in this setup, we do not make the output private intentionally as adding noise in the softmax vector may deceive the physician if the magnitude of noise is too high. Next, it also causes a drop in utility. Finally, as we only communicate the final label and the LDP-fied explanation with the patients (subject to physicians’ approval), we do not need to disclose this information and we securely communicate the same over an encrypted channel with the concerned physician.

Generating Privacy Preserving Explanation: The system then proceeds to the explanation generation phase, where post-hoc explainers analyze the model’s decision. These explanations undergo a critical privacy-preserving transformation in what we term the *noise chamber*. Here, carefully calibrated noise is injected into the explanations to make the generated explanations LDP. The noise calibration is based on our theoretical findings about sensitivity patterns in DP models, ensuring that the added noise preserves the essential aspects of the explanations while providing privacy guarantees.

Quality Assessment and Information Delivery: After noise injection, the system performs an SSIM analysis between the LDP-fied explanations and their original counterparts. This quality check ensures that the privacy-preserving mechanisms haven’t significantly degraded the explanation quality. The system prioritizes the top-K (for our case, $K = 1 - 2$) explanations. This is a crucial step as explanations which are severely degraded (say SSIM is in negative) should be discarded to save the time and effort of the concerned physician(s). These selected explanations, along with the model’s predictions, over the encrypted channels, are securely communicated to the concerned physician(s).

Final Communication Protocol: Once the concerned physician(s) formally reviews the prediction and explanations, we communicate the same to the patients subject to concerned physician(s)’ approval.

10 Related Work

Privacy-preserving machine learning (PPML). PPML is a critical component for RTP and includes a variety of techniques designed to safeguard individuals’ data while enabling meaningful machine learning analyses. Key methods in PPML include Differential Privacy (DP) Dwork et al. (2014); Abadi et al. (2016), Federated Learning (FL) McMahan et al. (2017); Kaissis et al. (2020); Konečný et al. (2016), Homomorphic Encryption (HE) Brand and Pradel (2023), and Secure Multi-Party Computation (SMPC) Zhou et al. (2024) to

20. we, after consulting with physicians from SRM University AP, have considered images from classes other than Pneumonia and TB such as Cardiomegaly, Aortic enlargement here as anomalous inputs; we have randomly taken 50 samples per class from Nguyen et al. (2022) dataset.

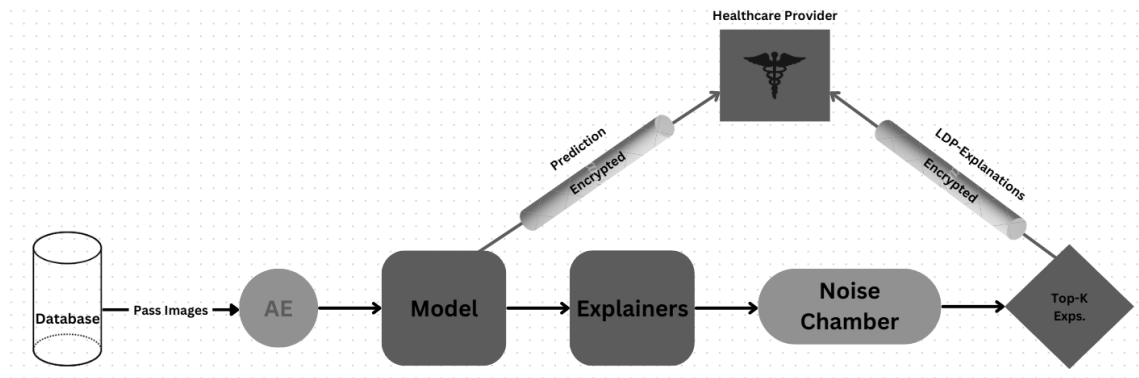


Figure 7: Outline of the Software

mention a few. DP is especially notable for ensuring that the inclusion or exclusion of any single data point has minimal impact on the results of computations, providing strong guarantees that sensitive information cannot be easily inferred from model outputs. FL enables decentralized training, allowing models to be trained on local devices without the need to share raw data. Homomorphic Encryption allows computations to be performed on encrypted data, while SMPC enables multiple parties to collaboratively train models without revealing their private data.

Among these approaches, DP is often regarded as the most suitable for many privacy-preserving applications due to its solid theoretical foundation and scalability. DP offers formal, quantifiable privacy guarantees, making it applicable across diverse domains. Unlike other methods, DP facilitates flexible trade-offs between privacy and utility by adjusting parameters like the noise scale, and it can be seamlessly integrated into a variety of machine learning algorithms. In comparison, techniques such as FL, HE, and SMPC offer privacy advantages but may introduce higher computational overheads and more complex infrastructure requirements Xu et al. (2021). These limitations can hinder their applicability in resource-constrained settings or in large-scale, real-time applications. Consequently, DP remains the preferred approach for balancing privacy protection with the efficient and scalable deployment of machine learning models. For a comprehensive review of PPML, we direct readers to the excellent survey by Boulemtafes et al. Boulemtafes et al. (2020).

Explainable machine learning (XAI). XAI is crucial for RTE. XAI methods are generally categorized into three types: local Ribeiro et al. (2016); Lundberg and Lee (2017); Sundararajan et al. (2017); Smilkov et al. (2017), global Ibrahim et al. (2019); Lundberg et al. (2020), and inherently interpretable models Ditz (2024); Molnar et al. (2020). Local explanations focus on providing insights into specific predictions for individual instances, while global explanations aim to clarify the overall behavior of the model across a range of examples. Inherently interpretable models, such as decision trees or linear models, are designed to be understandable from the outset. In this paper, we focus on local, post-hoc explainers (see Appendix C), which are particularly practical in industrial settings due to their “plug-and-play” nature. These methods do not require modifications to the model or its training process, making them highly adaptable in real-world applications Bhatt et al. (2020b).

These local explainers can be further divided into two categories: perturbation-based methods and gradient-based methods Saeed and Omlin (2023). Perturbation-based methods, such as LIME Ribeiro et al. (2016) and SHAP Lundberg and Lee (2017), analyze model predictions by altering the input and observing how the output changes. In contrast, gradient-based methods rely on the gradients of the model’s output with respect to the given inputs to generate explanations Saeed and Omlin (2023).

When evaluating the quality of explanations, key factors such as faithfulness, plausibility, and robustness are critical Zhou et al. (2021). Faithfulness refers to how accurately the explanation reflects the model’s actual decision-making process Lyu et al. (2024), while plausibility concerns how well the explanation aligns with human intuition or understanding Zhou et al. (2021); Lyu et al. (2024). Robustness measures the consistency of the explanation across small perturbations in the input or model Alvarez-Melis and Jaakkola (2018). Among these, faithfulness is widely regarded as the most important metric. An explanation that is not faithful to the model’s true behavior can mislead users, eroding trust in the system Lyu et al. (2024). While plausibility is important, it is insufficient by itself—an explanation that seems plausible to a human may still be unfaithful to the model’s actual behavior, which can ultimately deceive the end user Zhong et al. (2019). Therefore, faithfulness must remain the primary objective in XAI. However, measuring faithfulness presents its own challenges, and existing metrics are far from perfect, as discussed in Section 3.2. Even in domains like natural language processing, traditional erasure-based measures for evaluating faithfulness have proven flawed, leading to misleading conclusions about the quality of explanations, as noted in the recent work of Manna and Sett Manna and Sett (2024).

In this paper, we propose an alternative method for assessing the extent to which DP explanations can serve as a proxy for their non-DP counterparts. However, our mechanistic interpretation of DP models reveals that standard explainers are not well-suited for this context, due to the inherent differences between the nature of DP models and their non-DP counterparts.

However in this work, we did not consider model-agnostic perturbation-based explainers such as KernelSHAP, LIME, or Occlusion: other than their limited adaptation in computer vision tasks, Shokri et al. Shokri et al. (2021) criticized these methods for failing to follow the distribution of the training data and violating the data manifold hypothesis, which suggests that “data tend to lie near a low-dimensional manifold” Fefferman et al. (2016). Shokri et al. Shokri et al. (2021) further conjectured that this inherent shortcoming makes such methods fundamentally inappropriate for evaluating models with DP models. Subsequently, Kumar et al. Kumar et al. (2020) and Sundararajan et al. Sundararajan and Najmi (2020) also found that perturbation-based methods often operate outside the data’s true distribution, potentially leading to inaccurate or misleading explanations. While we did consider **Grad-Shap**, which can be seen as an approximation of **Integrated Gradients** by computing expectations of gradients over different baselines²¹, we found that none of the selected explainers were effective or reliable when applied to DP models. This underscores the challenges of using traditional explainability techniques in the context of private models.

Privacy-preserving explainable AI (PPXAI). PPXAI methods have only recently begun to emerge, with approaches such as differentially private Locally Linear Maps (LLM)

21. Captum

Harder et al. (2020), differentially private feature-based model explanations Patel et al. (2022), differentially private counterfactual explanations Mochaourab et al. (2021). For a comprehensive overview of PPXAI, we direct readers to the comprehensive survey by Nguyen et al. Nguyen et al. (2024). However, these methods are not included in our analysis due to their limited adoption and lack of extensive evaluation on critical aspects other than privacy preservation such as explanation quality and faithfulness, unlike the more widely used explainability techniques considered in this study.

Recently, researchers have begun investigating the quality of explanations in privacy-preserving environments. Bozorgpanah et al. Bozorgpanah et al. (2022) generated private datasets (benchmark tabular datasets) using masking methods and compared the Shapley values Lundberg and Lee (2017) for test instances given the two models: trained on non private data and trained on private data. They found minimal effect on moderate protection. Lucieri et al. Lucieri et al. (2023) investigated the effect of DP training on concept-based explanations on biomedical datasets, and found that DP decreases average Concept Activation Vectors (CAV) accuracy and increases standard deviation; whereas Saifullah et al. (2024) has reported that differential privacy and federated learning may yield ‘noisy’ feature attribution score for post-hoc explainers. Berning et al. Berning et al. (2024) found that k-anonymity degrades the quality of counterfactual explanations on a tabular dataset. Bozorgpanah et al. Bozorgpanah and Torra (2024) generated private datasets (benchmark tabular datasets) using masking methods and noise addition and applied TreeSHAP to achieve plausible explanations.

Our work is distinct from all of these previous efforts, as we first establish the desiderata for DP explanations and then mechanistically explore why DP models are particularly challenging to explain using traditional post-hoc explainers. We not only investigate global DP and its inherent limitations for RTE but also explored local DP to generate proxy private explanations. While Lucieri et al. (2023) and Saifullah et al. (2024) focused on global DP, the rest of the existing literature has primarily worked with local DP and to the best of our knowledge we are the first one to mechanistically interpret the DP models and discovered why post-hoc explaienrs are inappropriate in this context.

Analysing neural network similarity. Analysing neural network similarity is crucial for interpreting and improving model behavior. This can be broadly classified into two main types Klabunde et al. (2024): (i) representational similarity (RS), which measures differences in intermediate layer activations Kornblith et al. (2019); Cui et al. (2022); Raghu et al. (2017); Li et al. (2015), and (ii) functional similarity, which evaluates discrepancies in model outputs Hsu and Calmon (2022); Milani Fard et al. (2016); Marx et al. (2020).

To investigate why DP models fail to accommodate common post-hoc explainers, we worked with RS to examine layer-wise changes in activations and their sensitivities. However, in such cases the similarity measures researchers employ adhere to specific invariances: Permutations, Orthogonal Transformations, Isotropic Scaling, Translations etc are to name a few. We have considered the mostly used set of invariances and chose CKA for measuring RS but CKA, by its design, comes with a few shortcomings as discussed in section 7. Consequently, we chose dCKA proposed by Cui et al. (2022) for our analysis. For a broader view on neural network similarity, we refer the readers to the wonderful survey by Klabunde et al. Klabunde et al. (2024).

11 Limitation of the Work

In this work, we primarily restricted our study to DP models, their activation patterns and their intrinsic behaviour. We have shown that an immediate consequence of the same is the non-functionality of famous gradient-based post-hoc explainers with the DP model. There can be different notions and setups for privacy-preserving machine learning and other classes of explainers are also there - we didn't consider them for this research. Also, the (un)fairness of DP models Fioretto et al. (2022) is not considered under the scope of this research.

12 Conclusion and Future Studies

We started our research with a simple question of whether we can achieve RTP and RTE *together*. We kept an eye on the pitfalls of commonly used evaluation metrics for explainability and proposed our desiderata and found that no commonly used gradient-based explainers are useful for private models. We investigate the activations inside a DP model and how the model is sensitive towards those; we discovered that the intrinsic behaviour of DP models is the key reason behind this. Our ‘mechanistic’ Saphra and Wiegreffe (2024) insights of the private models across different privacy guarantees highlight how DP training alters the internal representations and their sensitivities. It gives a fresh perspective on interpreting DP models and their behaviour from a nuanced angle. Lastly, we make use of LDP to achieve private explanations and conclude our study by outlining the pipeline for the industrial software for our use case that respects both RTP and RTE.

In future studies, we aim to go deeper into the sensitivity landscape of DP models by investigating second-order and higher-order derivatives of the model’s output w.r.t. representations. While our current analysis focused on first-order gradients, examining higher-order derivatives could potentially uncover richer structural patterns in the sensitivity space that aren’t immediately apparent through first-order analysis. This exploration is particularly intriguing as higher-order derivatives might capture more nuanced interactions between features and reveal how privacy constraints affect these complex relationships. Specifically, we want to analyze how the Hessian and higher-order tensors of DP models differ from their non-private counterparts, which could provide insights into more complicated behavioural patterns. Understanding these higher-order sensitivities could not only enhance our mechanistic interpretation of DP models but also potentially lead to more sophisticated XAI method(s) that capture intricate model behaviours subject to privacy guarantees. This direction is especially promising as it might reveal whether the privacy-induced changes in model behaviour have deeper structural implications beyond what is observable through first-order sensitivity analysis.

Acknowledgement

We are thankful to Jim Conant for the fruitful discussion on high-dimensional geometry. We are thankful to Yogesh Kumar, the co-author of dCKA Cui et al. (2022) for a productive discussion. We are also thankful to Dr. Venkata Abhinay Talasila from SRM University AP for his immense cooperation throughout.

References

Martin Abadi, Andy Chu, Ian Goodfellow, H. Brendan McMahan, Ilya Mironov, Kunal Talwar, and Li Zhang. Deep learning with differential privacy. In *Proceedings of the 2016 ACM SIGSAC Conference on Computer and Communications Security*, CCS'16. ACM, October 2016. doi: 10.1145/2976749.2978318. URL <http://dx.doi.org/10.1145/2976749.2978318>.

Julius Adebayo, Justin Gilmer, Michael Muelly, Ian Goodfellow, Moritz Hardt, and Been Kim. Sanity checks for saliency maps. *Advances in neural information processing systems*, 31, 2018.

Mohammed AA Al-qaness, Jie Zhu, Dalal AL-Alimi, Abdelghani Dahou, Saeed Hamood Alsamhi, Mohamed Abd Elaziz, and Ahmed A Ewees. Chest x-ray images for lung disease detection using deep learning techniques: A comprehensive survey. *Archives of Computational Methods in Engineering*, pages 1–35, 2024.

David Alvarez-Melis and Tommi S. Jaakkola. On the robustness of interpretability methods, 2018. URL <https://arxiv.org/abs/1806.08049>.

Marco Ancona, Enea Ceolini, Cengiz Öztireli, and Markus Gross. Towards better understanding of gradient-based attribution methods for deep neural networks. *arXiv preprint arXiv:1711.06104*, 2017.

Anna Arias-Duart, Ferran Parés, Dario Garcia-Gasulla, and Victor Giménez-Ábalos. Focus! rating xai methods and finding biases. In *2022 IEEE International Conference on Fuzzy Systems (FUZZ-IEEE)*, pages 1–8. IEEE, 2022.

Sebastian Bach, Alexander Binder, Grégoire Montavon, Frederick Klauschen, Klaus-Robert Müller, and Wojciech Samek. On pixel-wise explanations for non-linear classifier decisions by layer-wise relevance propagation. *PloS one*, 10(7):e0130140, 2015.

Sebastian Rodriguez Beltran, Marlon Tobaben, Joonas Jälkö, Niki Loppi, and Antti Honkela. Towards efficient and scalable training of differentially private deep learning. *arXiv preprint arXiv:2406.17298*, 2024.

Kamal Berahmand, Fatemeh Daneshfar, Elaheh Sadat Salehi, Yuefeng Li, and Yue Xu. Autoencoders and their applications in machine learning: a survey. *Artificial Intelligence Review*, 57(2):28, 2024.

Sjoerd Berning, Vincent Dunning, Dayana Spagnuelo, Thijs Veugen, and Jasper van der Waa. The trade-off between privacy & quality for counterfactual explanations. In *Proceedings of the 19th International Conference on Availability, Reliability and Security*, pages 1–9, 2024.

Umang Bhatt, Adrian Weller, and José MF Moura. Evaluating and aggregating feature-based model explanations. *arXiv preprint arXiv:2005.00631*, 2020a.

Umang Bhatt, Alice Xiang, Shubham Sharma, Adrian Weller, Ankur Taly, Yunhan Jia, Joydeep Ghosh, Ruchir Puri, José M. F. Moura, and Peter Eckersley. Explainable machine learning in deployment, 2020b. URL <https://arxiv.org/abs/1909.06342>.

Robi Bhattacharjee and Kamalika Chaudhuri. When are non-parametric methods robust? In *International Conference on Machine Learning*, pages 832–841. PMLR, 2020.

Alberto Blanco-Justicia, David Sánchez, Josep Domingo-Ferrer, and Krishnamurty Muralidhar. A critical review on the use (and misuse) of differential privacy in machine learning. *ACM Computing Surveys*, 55(8):1–16, December 2022. ISSN 1557-7341. doi: 10.1145/3547139. URL <http://dx.doi.org/10.1145/3547139>.

Revoti Prasad Bora, Kiran Raja, Philipp Terhörst, Raymond Veldhuis, and Raghavendra Ramachandra. Why sanity check for saliency metrics fails?, 2024. URL <https://openreview.net/forum?id=Pev2ufTzMv>.

Amine Boulemtafes, Abdelouahid Derhab, and Yacine Challal. A review of privacy-preserving techniques for deep learning. *Neurocomputing*, 384:21–45, 2020.

Aso Bozorgpanah and Vicenç Torra. Explainable machine learning models with privacy. *Progress in Artificial Intelligence*, 13(1):31–50, 2024.

Aso Bozorgpanah, Vicenç Torra, and Laya Aliahmadipour. Privacy and explainability: The effects of data protection on shapley values. *Technologies*, 10(6):125, 2022.

Michael Brand and Gaëtan Pradel. Practical privacy-preserving machine learning using fully homomorphic encryption. Cryptology ePrint Archive, Paper 2023/1320, 2023. URL <https://eprint.iacr.org/2023/1320>.

Vanessa Buhrmester, David Münch, and Michael Arens. Analysis of explainers of black box deep neural networks for computer vision: A survey. *Machine Learning and Knowledge Extraction*, 3(4):966–989, 2021.

Captum. Captum · Model Interpretability for PyTorch. URL https://captum.ai/api/gradient_shap.html.

Prasad Chalasani, Jiefeng Chen, Amrita Roy Chowdhury, Xi Wu, and Somesh Jha. Concise explanations of neural networks using adversarial training. In *International Conference on Machine Learning*, pages 1383–1391. PMLR, 2020.

Chun-Hao Chang, Elliot Creager, Anna Goldenberg, and David Duvenaud. Explaining image classifiers by counterfactual generation. *arXiv preprint arXiv:1807.08024*, 2018.

Tianyu Cui, Yogesh Kumar, Pekka Marttinen, and Samuel Kaski. Deconfounded representation similarity for comparison of neural networks. *Advances in Neural Information Processing Systems*, 35:19138–19151, 2022.

Sanjoy Dasgupta, Nave Frost, and Michal Moshkovitz. Framework for evaluating faithfulness of local explanations. In *International Conference on Machine Learning*, pages 4794–4815. PMLR, 2022.

MohammadReza Davari, Stefan Horoi, Amine Natik, Guillaume Lajoie, Guy Wolf, and Eugene Belilovsky. Reliability of cka as a similarity measure in deep learning. *arXiv preprint arXiv:2210.16156*, 2022.

Jonas Ditz. *Towards Inherently Interpretable Machine Learning for Healthcare*. PhD thesis, Universität Tübingen, 2024.

Shi Dong, Ping Wang, and Khushnood Abbas. A survey on deep learning and its applications. *Computer Science Review*, 40:100379, 2021.

Cynthia Dwork, Aaron Roth, et al. The algorithmic foundations of differential privacy. *Foundations and Trends® in Theoretical Computer Science*, 9(3–4):211–407, 2014.

Izegbua E. Ihongbe, Shereen Fouad, Taha F. Mahmoud, Arvind Rajasekaran, and Bahadar Bhatia. Evaluating explainable artificial intelligence (xai) techniques in chest radiology imaging through a human-centered lens. *Plos one*, 19(10):e0308758, 2024.

Theodore Evans, Carl Orge Retzlaff, Christian Geißler, Michaela Kargl, Markus Plass, Heimo Müller, Tim-Rasmus Kiehl, Norman Zerbe, and Andreas Holzinger. The explainability paradox: Challenges for xai in digital pathology. *Future Generation Computer Systems*, 133:281–296, 2022.

Liyue Fan. Image pixelization with differential privacy. In *Data and Applications Security and Privacy XXXII: 32nd Annual IFIP WG 11.3 Conference, DBSec 2018, Bergamo, Italy, July 16–18, 2018, Proceedings 32*, pages 148–162. Springer, 2018.

Charles Fefferman, Sanjoy Mitter, and Hariharan Narayanan. Testing the manifold hypothesis. *Journal of the American Mathematical Society*, 29(4):983–1049, 2016.

Ferdinando Fioretto, Cuong Tran, Pascal Van Hentenryck, and Keyu Zhu. Differential privacy and fairness in decisions and learning tasks: A survey. *arXiv preprint arXiv:2202.08187*, 2022.

Matt Fredrikson, Somesh Jha, and Thomas Ristenpart. Model inversion attacks that exploit confidence information and basic countermeasures. In *Proceedings of the 22nd ACM SIGSAC conference on computer and communications security*, pages 1322–1333, 2015.

Alex Gaudio. *Explainable Deep Machine Learning for Medical Image Analysis*. PhD thesis, Carnegie Mellon University, 2023.

Arthur Gretton, Kenji Fukumizu, Choon Teo, Le Song, Bernhard Schölkopf, and Alex Smola. A kernel statistical test of independence. *Advances in neural information processing systems*, 20, 2007.

Arthur Gretton, Karsten M. Borgwardt, Malte J. Rasch, Bernhard Schölkopf, and Alexander Smola. A kernel two-sample test. *Journal of Machine Learning Research*, 13(25):723–773, 2012. URL <http://jmlr.org/papers/v13/gretton12a.html>.

Fabian Gwinner, Christoph Tomitzka, and Axel Winkelmann. Comparing expert systems and their explainability through similarity. *Decision Support Systems*, 182:114248, 2024.

Tessa Han, Suraj Srinivas, and Himabindu Lakkaraju. Which explanation should i choose? a function approximation perspective to characterizing post hoc explanations. *Advances in neural information processing systems*, 35:5256–5268, 2022.

Frederik Harder, Matthias Bauer, and Mijung Park. Interpretable and differentially private predictions. In *Proceedings of the AAAI Conference on Artificial Intelligence*, volume 34, pages 4083–4090, 2020.

Peter Hase, Harry Xie, and Mohit Bansal. The out-of-distribution problem in explainability and search methods for feature importance explanations. *Advances in neural information processing systems*, 34:3650–3666, 2021.

Johannes Haug, Stefan Zürn, Peter El-Jiz, and Gjergji Kasneci. On baselines for local feature attributions. *arXiv preprint arXiv:2101.00905*, 2021.

Kaiming He, Xiangyu Zhang, Shaoqing Ren, and Jian Sun. Deep residual learning for image recognition. In *Proceedings of the IEEE conference on computer vision and pattern recognition*, pages 770–778, 2016.

Anna Hedström, Leander Weber, Daniel Krakowczyk, Dilyara Bareeva, Franz Motzkus, Wojciech Samek, Sebastian Lapuschkin, and Marina M-C Höhne. Quantus: An explainable ai toolkit for responsible evaluation of neural network explanations and beyond. *Journal of Machine Learning Research*, 24(34):1–11, 2023.

Hsiang Hsu and Flavio Calmon. Rashomon capacity: A metric for predictive multiplicity in classification. *Advances in Neural Information Processing Systems*, 35:28988–29000, 2022.

Hongsheng Hu, Zoran Salcic, Lichao Sun, Gillian Dobbie, Philip S Yu, and Xuyun Zhang. Membership inference attacks on machine learning: A survey. *ACM Computing Surveys (CSUR)*, 54(11s):1–37, 2022.

Gao Huang, Zhuang Liu, Laurens Van Der Maaten, and Kilian Q Weinberger. Densely connected convolutional networks. In *Proceedings of the IEEE conference on computer vision and pattern recognition*, pages 4700–4708, 2017.

Tobias Huber, Katharina Weitz, Elisabeth André, and Ofra Amir. Local and global explanations of agent behavior: Integrating strategy summaries with saliency maps. *Artificial Intelligence*, 301:103571, 2021.

Mark Ibrahim, Melissa Louie, Ceena Modarres, and John Paisley. Global explanations of neural networks: Mapping the landscape of predictions. In *Proceedings of the 2019 AAAI/ACM Conference on AI, Ethics, and Society*, pages 279–287, 2019.

Tanzina Taher Ifty, Saleh Ahmed Shafin, Shoeb Mohammad Shahriar, and Tashfia Towhid. Explainable lung disease classification from chest x-ray images utilizing deep learning and xai. *arXiv preprint arXiv:2404.11428*, 2024.

Adam Ivankay, Ivan Girardi, Chiara Marchiori, and Pascal Frossard. Fooling explanations in text classifiers. *arXiv preprint arXiv:2206.03178*, 2022.

Alon Jacovi and Yoav Goldberg. Towards faithfully interpretable nlp systems: How should we define and evaluate faithfulness? *arXiv preprint arXiv:2004.03685*, 2020.

Alon Jacovi and Yoav Goldberg. Aligning faithful interpretations with their social attribution. *Transactions of the Association for Computational Linguistics*, 9:294–310, 2021.

Dominik Janzing, Lenon Minorics, and Patrick Blöbaum. Feature relevance quantification in explainable ai: A causal problem. In *International Conference on artificial intelligence and statistics*, pages 2907–2916. PMLR, 2020.

Arnulf Jentzen, Benno Kuckuck, and Philippe von Wurstemberger. Mathematical introduction to deep learning: Methods, implementations, and theory, 2023. URL <https://arxiv.org/abs/2310.20360>.

Zhanglong Ji, Zachary C Lipton, and Charles Elkan. Differential privacy and machine learning: a survey and review. *arXiv preprint arXiv:1412.7584*, 2014.

Yiming Ju, Yuanzhe Zhang, Zhao Yang, Zhongtao Jiang, Kang Liu, and Jun Zhao. Logic traps in evaluating attribution scores. *arXiv preprint arXiv:2109.05463*, 2021.

Georgios A Kaassis, Marcus R Makowski, Daniel Rückert, and Rickmer F Braren. Secure, privacy-preserving and federated machine learning in medical imaging. *Nature Machine Intelligence*, 2(6):305–311, 2020.

Nazish Khalid, Adnan Qayyum, Muhammad Bilal, Ala Al-Fuqaha, and Junaid Qadir. Privacy-preserving artificial intelligence in healthcare: Techniques and applications. *Computers in Biology and Medicine*, 158:106848, 2023.

Max Klabunde, Tobias Schumacher, Markus Strohmaier, and Florian Lemmerich. Similarity of neural network models: A survey of functional and representational measures, 2024. URL <https://arxiv.org/abs/2305.06329>.

Maximilian Kohlbrenner, Alexander Bauer, Shinichi Nakajima, Alexander Binder, Wojciech Samek, and Sebastian Lapuschkin. Towards best practice in explaining neural network decisions with lrp. In *2020 International Joint Conference on Neural Networks (IJCNN)*, pages 1–7. IEEE, 2020.

Narine Kokhlikyan, Vivek Miglani, Bilal Alsallakh, Miguel Martin, and Orion Reblitz-Richardson. Investigating sanity checks for saliency maps with image and text classification. *arXiv preprint arXiv:2106.07475*, 2021.

Jakub Konečný, H. Brendan McMahan, Daniel Ramage, and Peter Richtárik. Federated optimization: Distributed machine learning for on-device intelligence, 2016. URL <https://arxiv.org/abs/1610.02527>.

Simon Kornblith, Mohammad Norouzi, Honglak Lee, and Geoffrey Hinton. Similarity of neural network representations revisited. In *International conference on machine learning*, pages 3519–3529. PMLR, 2019.

Satyapriya Krishna, Tessa Han, Alex Gu, Javin Pombra, Shahin Jabbari, Steven Wu, and Himabindu Lakkaraju. The disagreement problem in explainable machine learning: A practitioner’s perspective, 2022. URL <https://arxiv.org/abs/2202.01602>.

I Elizabeth Kumar, Suresh Venkatasubramanian, Carlos Scheidegger, and Sorelle Friedler. Problems with shapley-value-based explanations as feature importance measures. In *International conference on machine learning*, pages 5491–5500. PMLR, 2020.

Junbing Li, Changqing Zhang, Joey Tianyi Zhou, Huazhu Fu, Shuyin Xia, and Qinghua Hu. Deep-lift: Deep label-specific feature learning for image annotation. *IEEE transactions on Cybernetics*, 52(8):7732–7741, 2021.

Xuhong Li, Mengnan Du, Jiamin Chen, Yekun Chai, Himabindu Lakkaraju, and Haoyi Xiong. M4: A unified xai benchmark for faithfulness evaluation of feature attribution methods across metrics, modalities and models. *Advances in Neural Information Processing Systems*, 36:1630–1643, 2023.

Yixuan Li, Jason Yosinski, Jeff Clune, Hod Lipson, and John Hopcroft. Convergent learning: Do different neural networks learn the same representations? *arXiv preprint arXiv:1511.07543*, 2015.

Huiting Liu, Siddharth Patwardhan, Peter Grasch, Sachin Agarwal, et al. Model stability with continuous data updates. *arXiv preprint arXiv:2201.05692*, 2022.

Andrew Lowy, Zhuohang Li, Jing Liu, Toshiaki Koike-Akino, Kieran Parsons, and Ye Wang. Why does differential privacy with large epsilon defend against practical membership inference attacks? *arXiv preprint arXiv:2402.09540*, 2024.

Adriano Lucieri, Andreas Dengel, and Sheraz Ahmed. Translating theory into practice: assessing the privacy implications of concept-based explanations for biomedical ai. *Frontiers in Bioinformatics*, 3:1194993, 2023.

Scott M Lundberg and Su-In Lee. A unified approach to interpreting model predictions. *Advances in neural information processing systems*, 30, 2017.

Scott M Lundberg, Gabriel Erion, Hugh Chen, Alex DeGrave, Jordan M Prutkin, Bala Nair, Ronit Katz, Jonathan Himmelfarb, Nisha Bansal, and Su-In Lee. From local explanations to global understanding with explainable ai for trees. *Nature machine intelligence*, 2(1): 56–67, 2020.

Qing Lyu, Marianna Apidianaki, and Chris Callison-Burch. Towards faithful model explanation in nlp: A survey. *Computational Linguistics*, pages 1–67, 2024.

Supriya Manna and Niladri Sett. Faithfulness and the notion of adversarial sensitivity in nlp explanations. *arXiv preprint arXiv:2409.17774*, 2024.

Charles Marx, Flavio Calmon, and Berk Ustun. Predictive multiplicity in classification. In *International Conference on Machine Learning*, pages 6765–6774. PMLR, 2020.

Shiona McCallum. CHATGPT banned in Italy over privacy concerns, 2023. URL <https://www.bbc.com/news/technology-65139406>.

Brendan McMahan, Eider Moore, Daniel Ramage, Seth Hampson, and Blaise Aguera y Arcas. Communication-Efficient Learning of Deep Networks from Decentralized Data. In Aarti Singh and Jerry Zhu, editors, *Proceedings of the 20th International Conference on Artificial Intelligence and Statistics*, volume 54 of *Proceedings of Machine Learning Research*, pages 1273–1282. PMLR, 20–22 Apr 2017.

Mahdi Milani Fard, Quentin Cormier, Kevin Canini, and Maya Gupta. Launch and iterate: Reducing prediction churn. *Advances in Neural Information Processing Systems*, 29, 2016.

Miquel Miró-Nicolau, Antoni Jaume-i Capó, and Gabriel Moyà-Alcover. A comprehensive study on fidelity metrics for xai. *arXiv preprint arXiv:2401.10640*, 2024.

Saumitra Mishra, Sanghamitra Dutta, Jason Long, and Daniele Magazzeni. A survey on the robustness of feature importance and counterfactual explanations. *arXiv preprint arXiv:2111.00358*, 2021.

Rami Mochaourab, Sugandh Sinha, Stanley Greenstein, and Panagiotis Papapetrou. Robust counterfactual explanations for privacy-preserving svm. In *International Conference on Machine Learning (ICML 2021), Workshop on Socially Responsible Machine Learning*, 2021.

Ali Mohammadi and Giorgis Petridis. Almost orthogonal subsets of vector spaces over finite fields. *European Journal of Combinatorics*, 103:103515, 2022. ISSN 0195-6698. doi: <https://doi.org/10.1016/j.ejc.2022.103515>. URL <https://www.sciencedirect.com/science/article/pii/S0195669822000117>.

Christoph Molnar, Giuseppe Casalicchio, and Bernd Bischl. Interpretable machine learning—a brief history, state-of-the-art and challenges. In *Joint European conference on machine learning and knowledge discovery in databases*, pages 417–431. Springer, 2020.

Grégoire Montavon, Alexander Binder, Sebastian Lapuschkin, Wojciech Samek, and Klaus-Robert Müller. Layer-wise relevance propagation: an overview. *Explainable AI: interpreting, explaining and visualizing deep learning*, pages 193–209, 2019.

Vankamamidi S Naresh, Muthusamy Thamarai, and VVL Divakar Allavarpu. Privacy-preserving deep learning in medical informatics: applications, challenges, and solutions. *Artificial Intelligence Review*, 56(Suppl 1):1199–1241, 2023.

National Institute of Allergy and Infectious Diseases. Niaid tb portal program dataset, n.d. URL <https://tbportals.niaid.nih.gov/>.

Michael Neely, Stefan F Schouten, Maurits JR Bleeker, and Ana Lucic. Order in the court: Explainable ai methods prone to disagreement. *arXiv preprint arXiv:2105.03287*, 2021.

Asif Ahmed Neloy and Maxime Turgeon. A comprehensive study of auto-encoders for anomaly detection: Efficiency and trade-offs. *Machine Learning with Applications*, page 100572, 2024.

An-phi Nguyen and María Rodríguez Martínez. On quantitative aspects of model interpretability. *arXiv preprint arXiv:2007.07584*, 2020.

Ha Q Nguyen, Khanh Lam, Linh T Le, Hieu H Pham, Dat Q Tran, Dung B Nguyen, Dung D Le, Chi M Pham, Hang TT Tong, Diep H Dinh, et al. Vindr-cxr: An open dataset of chest x-rays with radiologist’s annotations. *Scientific Data*, 9(1):429, 2022.

Thanh Tam Nguyen, Thanh Trung Huynh, Zhao Ren, Thanh Toan Nguyen, Phi Le Nguyen, Hongzhi Yin, and Quoc Viet Hung Nguyen. A survey of privacy-preserving model explanations: Privacy risks, attacks, and countermeasures, 2024. URL <https://arxiv.org/abs/2404.00673>.

Daryna Oliynyk, Rudolf Mayer, and Andreas Rauber. I know what you trained last summer: A survey on stealing machine learning models and defences. *ACM Computing Surveys*, 55(14s):1–41, 2023.

Nicolas Papernot, Shuang Song, Ilya Mironov, Ananth Raghunathan, Kunal Talwar, and Úlfar Erlingsson. Scalable private learning with pate, 2018. URL <https://arxiv.org/abs/1802.08908>.

Neel Patel, Reza Shokri, and Yair Zick. Model explanations with differential privacy. In *Proceedings of the 2022 ACM Conference on Fairness, Accountability, and Transparency*, pages 1895–1904, 2022.

Vitali Petsiuk, Abir Das, and Kate Saenko. Rise: Randomized input sampling for explanation of black-box models. *arXiv preprint arXiv:1806.07421*, 2018.

Natalia Ponomareva, Hussein Hazimeh, Alex Kurakin, Zheng Xu, Carson Denison, H. Brendan McMahan, Sergei Vassilvitskii, Steve Chien, and Abhradeep Guha Thakurta. How to dp-fy ml: A practical guide to machine learning with differential privacy. *Journal of Artificial Intelligence Research*, 77:1113–1201, July 2023. ISSN 1076-9757. doi: 10.1613/jair.1.14649. URL <http://dx.doi.org/10.1613/jair.1.14649>.

Shiva prasad Koyyada and Thipendra P Singh. An explainable artificial intelligence model for identifying local indicators and detecting lung disease from chest x-ray images. *Healthcare Analytics*, 4:100206, 2023.

Giovanni Puccetti. Measuring linear correlation between random vectors. *Information Sciences*, 607:1328–1347, 2022.

Luis Bernardo Pulido-Gaytan, Andrei Tchernykh, Jorge M Cortés-Mendoza, Mikhail Babenko, and Gleb Radchenko. A survey on privacy-preserving machine learning with fully homomorphic encryption. In *Latin American High Performance Computing Conference*, pages 115–129. Springer, 2020.

Maithra Raghu, Justin Gilmer, Jason Yosinski, and Jascha Sohl-Dickstein. Svcca: Singular vector canonical correlation analysis for deep learning dynamics and interpretability. *Advances in neural information processing systems*, 30, 2017.

Tawsifur Rahman, Amith Khandakar, Muhammad Abdul Kadir, Khandaker Rejaul Islam, Khandakar F Islam, Rashid Mazhar, Tahir Hamid, Mohammad Tariqul Islam, Saad Kashem, Zaid Bin Mahbub, et al. Reliable tuberculosis detection using chest x-ray with deep learning, segmentation and visualization. *Ieee Access*, 8:191586–191601, 2020.

Marco Tulio Ribeiro, Sameer Singh, and Carlos Guestrin. ” why should i trust you?” explaining the predictions of any classifier. In *Proceedings of the 22nd ACM SIGKDD international conference on knowledge discovery and data mining*, pages 1135–1144, 2016.

Laura Rieger and Lars Kai Hansen. Irof: a low resource evaluation metric for explanation methods. *arXiv preprint arXiv:2003.08747*, 2020.

Maria Rigaki and Sebastian Garcia. A survey of privacy attacks in machine learning. *ACM Computing Surveys*, 56(4):1–34, November 2023. ISSN 1557-7341. doi: 10.1145/3624010. URL <http://dx.doi.org/10.1145/3624010>.

Saumendu Roy, Gabriel Laberge, Banani Roy, Foutse Khomh, Amin Nikanjam, and Saikat Mondal. Why don’t xai techniques agree? characterizing the disagreements between post-hoc explanations of defect predictions. In *2022 IEEE International Conference on Software Maintenance and Evolution (ICSME)*, pages 444–448. IEEE, 2022.

Cynthia Rudin, Chaofan Chen, Zhi Chen, Haiyang Huang, Lesia Semenova, and Chudi Zhong. Interpretable machine learning: Fundamental principles and 10 grand challenges, 2021. URL <https://arxiv.org/abs/2103.11251>.

Waddah Saeed and Christian Omelin. Explainable ai (xai): A systematic meta-survey of current challenges and future opportunities. *Knowledge-Based Systems*, 263:110273, 2023.

Saifullah Saifullah, Dominique Mercier, Adriano Lucieri, Andreas Dengel, and Sheraz Ahmed. The privacy-explainability trade-off: unravelling the impacts of differential privacy and federated learning on attribution methods. *Frontiers in Artificial Intelligence*, 7:1236947, 2024.

Wojciech Samek, Alexander Binder, Grégoire Montavon, Sebastian Lapuschkin, and Klaus-Robert Müller. Evaluating the visualization of what a deep neural network has learned. *IEEE transactions on neural networks and learning systems*, 28(11):2660–2673, 2016.

Wojciech Samek, Thomas Wiegand, and Klaus-Robert Müller. Explainable artificial intelligence: Understanding, visualizing and interpreting deep learning models, 2017. URL <https://arxiv.org/abs/1708.08296>.

Naomi Saphra and Sarah Wiegreffe. Mechanistic?, 2024. URL <https://arxiv.org/abs/2410.09087>.

Salih Sarp, Ferhat Ozgur Catak, Murat Kuzlu, Umit Cali, Huseyin Kusetogullari, Yanxiao Zhao, Gungor Ates, and Ozgur Guler. An xai approach for covid-19 detection using transfer learning with x-ray images. *Heliyon*, 9(4), 2023.

Pranshu Saxena, Sanjay Kumar Singh, Gyanendra Tiwary, Yush Mittal, and Ishika Jain. An artificial intelligence technique for covid-19 detection with explainability using lungs x-ray images. In *2022 IEEE International Conference on Distributed Computing and Electrical Circuits and Electronics (ICDCECE)*, pages 1–6. IEEE, 2022.

Ramprasaath R. Selvaraju, Michael Cogswell, Abhishek Das, Ramakrishna Vedantam, Devi Parikh, and Dhruv Batra. Grad-cam: Visual explanations from deep networks via gradient-based localization. *International Journal of Computer Vision*, 128(2):336–359, October 2019. ISSN 1573-1405. doi: 10.1007/s11263-019-01228-7. URL <http://dx.doi.org/10.1007/s11263-019-01228-7>.

Gil I Shamir and Lorenzo Coviello. Anti-distillation: Improving reproducibility of deep networks. *arXiv preprint arXiv:2010.09923*, 2020.

Prashant Sharma. Chest x-ray (covid-19 & pneumonia), 2020. URL <https://www.kaggle.com/datasets/prashant268/chest-xray-covid19-pneumonia>.

Reza Shokri, Martin Strobel, and Yair Zick. On the privacy risks of model explanations. In *Proceedings of the 2021 AAAI/ACM Conference on AI, Ethics, and Society*, pages 231–241, 2021.

Sanchit Sinha, Hanjie Chen, Arshdeep Sekhon, Yangfeng Ji, and Yanjun Qi. Perturbing inputs for fragile interpretations in deep natural language processing. *arXiv preprint arXiv:2108.04990*, 2021.

Leon Sixt, Maximilian Granz, and Tim Landgraf. When explanations lie: Why many modified bp attributions fail. In *International conference on machine learning*, pages 9046–9057. PMLR, 2020.

David B Skalak et al. The sources of increased accuracy for two proposed boosting algorithms. In *Proc. American Association for Artificial Intelligence, AAAI-96, Integrating Multiple Learned Models Workshop*, volume 1129, page 1133. Citeseer, 1996.

Daniel Smilkov, Nikhil Thorat, Been Kim, Fernanda Viégas, and Martin Wattenberg. Smoothgrad: removing noise by adding noise. *arXiv preprint arXiv:1706.03825*, 2017.

Pranav Subramani, Nicholas Vadivelu, and Gautam Kamath. Enabling fast differentially private sgd via just-in-time compilation and vectorization. *Advances in Neural Information Processing Systems*, 34:26409–26421, 2021.

Mukund Sundararajan and Amir Najmi. The many shapley values for model explanation. In *International conference on machine learning*, pages 9269–9278. PMLR, 2020.

Mukund Sundararajan, Ankur Taly, and Qiqi Yan. Axiomatic attribution for deep networks. In *International conference on machine learning*, pages 3319–3328. PMLR, 2017.

Vinith M Suriyakumar, Nicolas Papernot, Anna Goldenberg, and Marzyeh Ghassemi. Chasing your long tails: Differentially private prediction in health care settings. In *Proceedings of the 2021 ACM Conference on Fairness, Accountability, and Transparency*, pages 723–734, 2021.

Latanya Sweeney. Only you, your doctor, and many others may know. *Technology Science*, 2015092903(9):29, 2015.

Tala Talaei Khoei, Hadjar Ould Slimane, and Naima Kaabouch. Deep learning: Systematic review, models, challenges, and research directions. *Neural Computing and Applications*, 35(31):23103–23124, 2023.

Mingxing Tan and Quoc Le. Efficientnetv2: Smaller models and faster training. In *International conference on machine learning*, pages 10096–10106. PMLR, 2021.

Jonas Theiner, Eric Müller-Budack, and Ralph Ewerth. Interpretable semantic photo geolocation. In *Proceedings of the IEEE/CVF Winter Conference on Applications of Computer Vision*, pages 750–760, 2022.

Judith Jarvis Thomson. The right to privacy. *Philosophy & Public Affairs*, pages 295–314, 1975.

Nurislam Tursynbek, Aleksandr Petiushko, and Ivan Oseledets. Robustness threats of differential privacy. *arXiv preprint arXiv:2012.07828*, 2020.

Michael Veale, Reuben Binns, and Lilian Edwards. Algorithms that remember: model inversion attacks and data protection law. *Philosophical Transactions of the Royal Society A: Mathematical, Physical and Engineering Sciences*, 376(2133):20180083, 2018.

Kate Vredenburgh. The right to explanation. *Journal of Political Philosophy*, 30(2):209–229, 2022.

Kuan-Chieh Wang, Yan Fu, Ke Li, Ashish Khisti, Richard Zemel, and Alireza Makhzani. Variational model inversion attacks. *Advances in Neural Information Processing Systems*, 34:9706–9719, 2021.

Zhou Wang, Alan C Bovik, Hamid R Sheikh, and Eero P Simoncelli. Image quality assessment: from error visibility to structural similarity. *IEEE transactions on image processing*, 13(4):600–612, 2004.

A. D. Wyner. Random packings and coverings of the unit n-sphere. *The Bell System Technical Journal*, 46(9):2111–2118, 1967. doi: 10.1002/j.1538-7305.1967.tb04246.x.

Runhua Xu, Nathalie Baracaldo, and James Joshi. Privacy-preserving machine learning: Methods, challenges and directions. *arXiv preprint arXiv:2108.04417*, 2021.

Chih-Kuan Yeh, Cheng-Yu Hsieh, Arun Suggala, David I Inouye, and Pradeep K Ravikumar. On the (in) fidelity and sensitivity of explanations. *Advances in neural information processing systems*, 32, 2019.

Gal Yona and Daniel Greenfeld. Revisiting sanity checks for saliency maps. *arXiv preprint arXiv:2110.14297*, 2021.

Ashkan Yousefpour, Igor Shilov, Alexandre Sablayrolles, Davide Testuggine, Karthik Prasad, Mani Malek, John Nguyen, Sayan Ghosh, Akash Bharadwaj, Jessica Zhao, Graham Cormode, and Ilya Mironov. Opacus: User-friendly differential privacy library in pytorch, 2022. URL <https://arxiv.org/abs/2109.12298>.

Fadila Zerka, Samir Barakat, Sean Walsh, Marta Bogowicz, Ralph TH Leijenaar, Arthur Jochems, Benjamin Miraglio, David Townend, and Philippe Lambin. Systematic review of privacy-preserving distributed machine learning from federated databases in health care. *JCO clinical cancer informatics*, 4:184–200, 2020.

Jianming Zhang, Sarah Adel Bargal, Zhe Lin, Jonathan Brandt, Xiaohui Shen, and Stan Sclaroff. Top-down neural attention by excitation backprop. *International Journal of Computer Vision*, 126(10):1084–1102, 2018.

Yu Zheng, Wenchao Zhang, Yonggang Zhang, Wei Song, Kai Zhou, and Bo Han. Rethinking improved privacy-utility trade-off with pre-existing knowledge for dp training. *arXiv preprint arXiv:2409.03344*, 2024.

Ruiqi Zhong, Steven Shao, and Kathleen McKeown. Fine-grained sentiment analysis with faithful attention. *arXiv preprint arXiv:1908.06870*, 2019.

Ian Zhou, Farzad Tofigh, Massimo Piccardi, Mehran Abolhasan, Daniel Franklin, and Justin Lipman. Secure multi-party computation for machine learning: A survey. *IEEE Access*, 2024.

Jianlong Zhou, Amir H Gandomi, Fang Chen, and Andreas Holzinger. Evaluating the quality of machine learning explanations: A survey on methods and metrics. *Electronics*, 10(5):593, 2021.

Fei Zhu, Shijie Ma, Zhen Cheng, Xu-Yao Zhang, Zhaoxiang Zhang, and Cheng-Lin Liu. Open-world machine learning: A review and new outlooks, 2024. URL <https://arxiv.org/abs/2403.01759>.

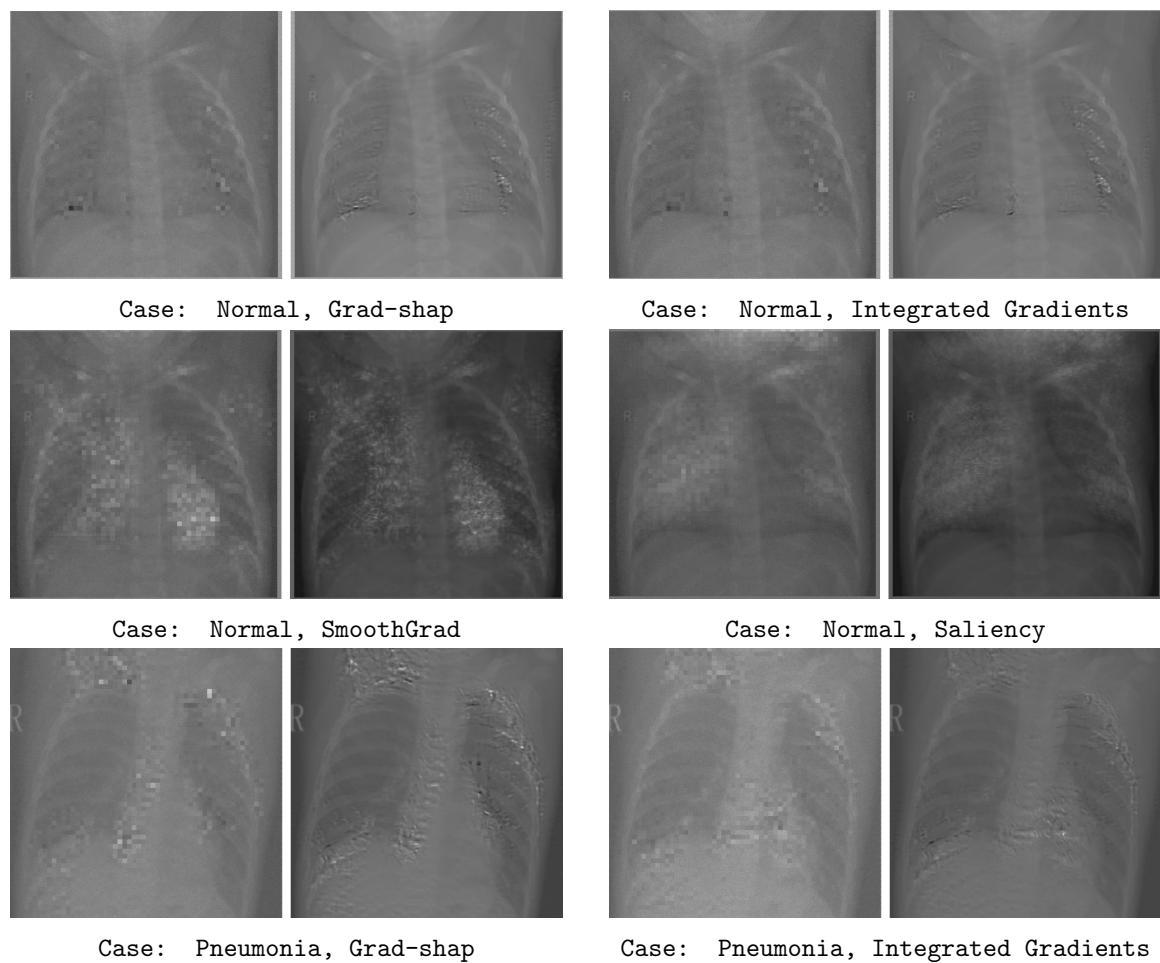
Appendix A.

Figure 8: For each plot, LDP explanation is on **Left** and Vanilla explanation is on **Right**

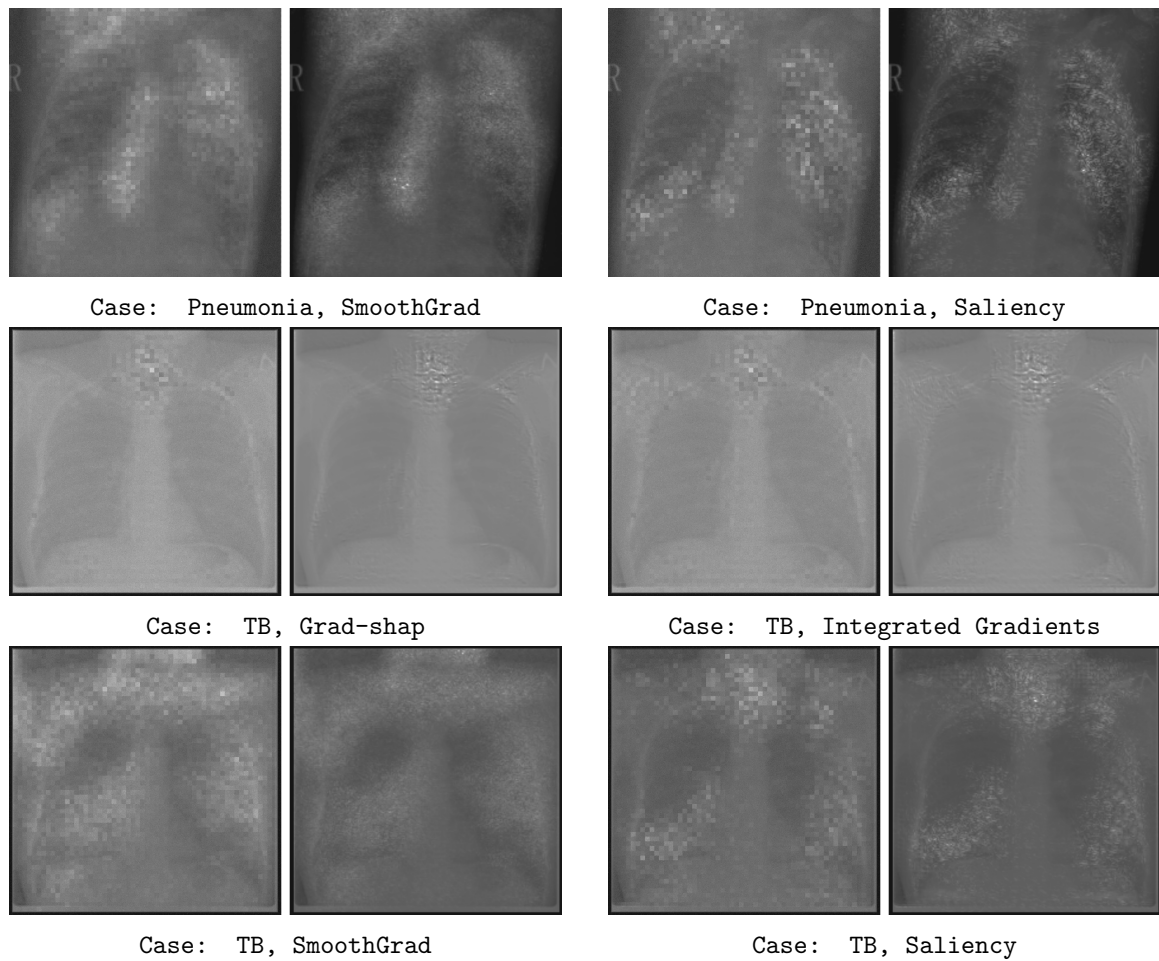


Figure 9: For each plot, LDP explanation is on **Left** and Vanilla explanation is on **Right**

Appendix B.

We trained ResNet-34 and DenseNet-121 models on the CIFAR-10 dataset using three ϵ values (4, 7, 10), as lower ϵ values resulted in harsh privacy-utility trade-off. We weren't able to train EfficientNet-v2 due to its exuberant computational requirement. We evaluated the models on the whole test set, consisting of total of 10,000 images. We train all models (both DP and non-DP counterparts) with the exact set of hyperparameters over 50 epochs. For brevity, we report $Acc_{\mathcal{M}}$ (Table 2), $Acc_{\mathcal{M}'/\mathcal{M}}$, and $-\times-$ taking all classes together for *Perf Comp.* and *Agreement* in Figure 12.

However, in this case as well **Integrated Gradients** and **Grad-Shap** yield 30% as mean DS score and the rest of the explainers also do not obtain $PIS_{Avg} > 0.3$ (Figure 12). Furthermore, here also we do not find any (apparent) PIS_{Avg} follows with *Perf Comp.* and/or *Agreement*. All in all, the results from our primary experiment are sufficiently comparable here as well. We will release the weights of these models upon publication.

For ResNet-34, we observed that sensitivity is independent across all layers for $\epsilon = 10$. However, only the last 2-3 layers for other ϵ values for ResNet-34 exhibited independent sensitivity. It indicates that independent sensitivity even in the last few layers can potentially make the explanations incomparable across ϵ values. In contrast, for DenseNet-121, independent sensitivity was consistently observed for all layers across all ϵ . For both types of models, we obtained fewer than 5-7% of layers where we couldn't reject the null hypothesis for independence of representation. We have reported the dCKA heatmap for DenseNet-121 and ResNet-34 models in figure 11, 10 respectively. Notably, the final layer for both ResNet-34 and DenseNet-121 consistently demonstrated independent sensitivity, rendering **Grad-CAM** unsuitable for generating comparable explanations. Consequently, we focused on other explainability methods in Figure 12.

Model	Acc (%)
DenseNet-121	72.82
ResNet-34	66.61

Table 2: Non-private models' accuracy

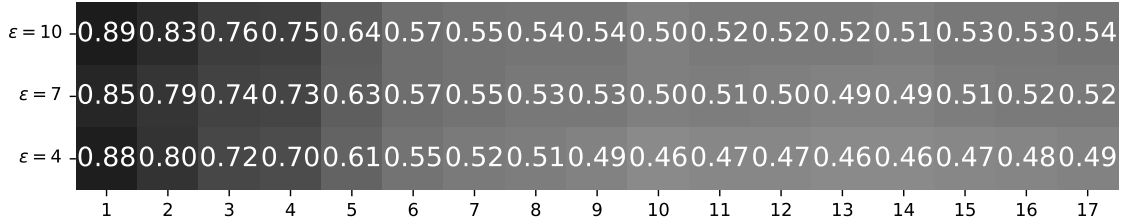


Figure 10: dCKA heatmap for ResNet-34 for CIFAR-10.

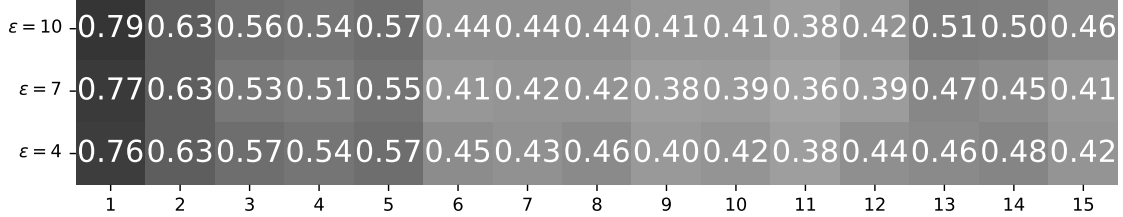
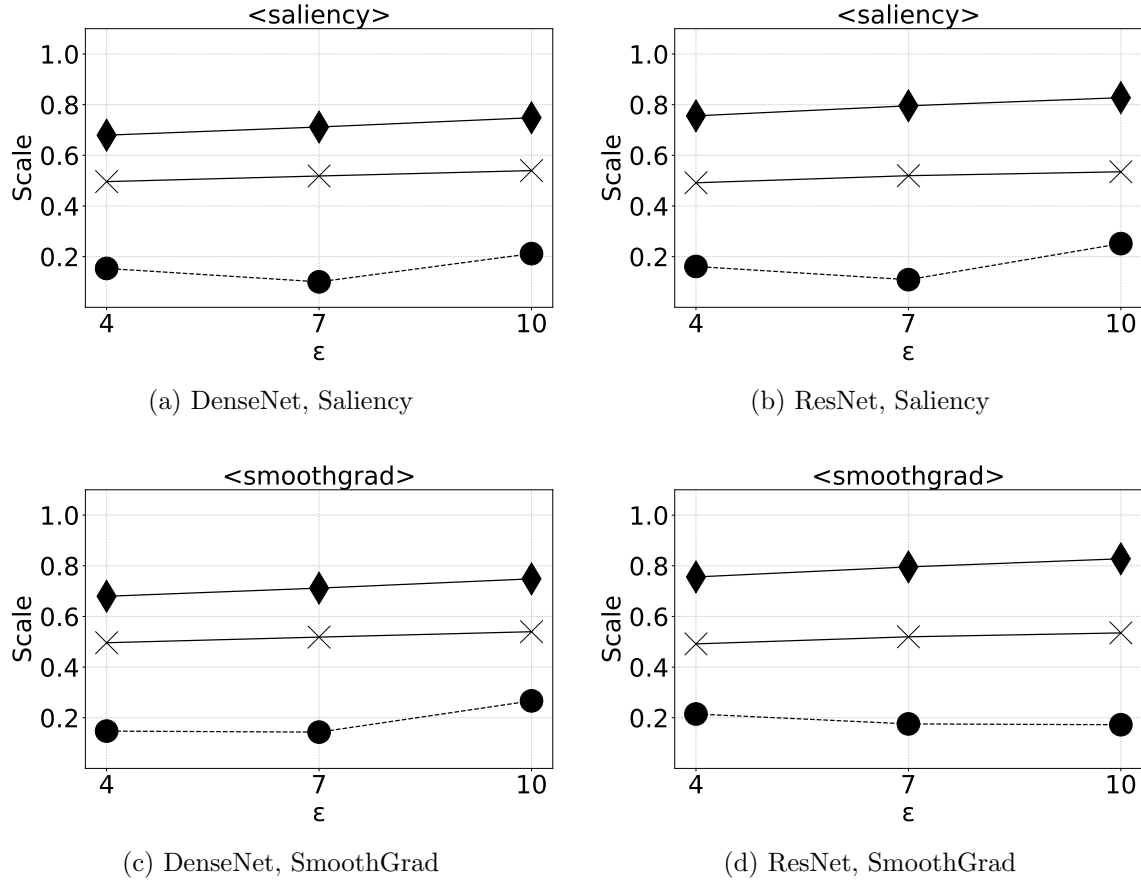


Figure 11: dCKA heatmap for DenseNet-121 for CIFAR-10.

Figure 12: Analysis on CIFAR-10: -●- for PIS_{Avg} , -◆- for $Acc_{M'/M}$, and - × - for $Agreement$ between non-private and private model pair.

Appendix C.

LIME (Local Interpretable Model-Agnostic Explanations): LIME Ribeiro et al. (2016) approximates a complex model locally using a simpler interpretable model (e.g., linear regression). For an input x , LIME generates perturbed versions of x and calculates the corresponding predictions to fit a local surrogate model. Mathematically, LIME solves the

following optimization problem:

$$\arg \min_{g \in G} \mathcal{L}(f, g, \pi_x) + \Omega(g),$$

where f is the original model, g is the interpretable surrogate model, π_x is a proximity measure to x , and $\Omega(g)$ ensures simplicity of g .

SHAP (SHapley Additive exPlanations): SHAP Lundberg and Lee (2017) explains model predictions based on cooperative game theory. For a prediction $f(x)$, SHAP attributes contributions to each feature using Shapley values:

$$\phi_i = \sum_{S \subseteq N \setminus \{i\}} \frac{|S|!(|N| - |S| - 1)!}{|N|!} [f(S \cup \{i\}) - f(S)],$$

where N is the set of all features, S is a subset of features, and $f(S)$ is the model's prediction with features in S included.

Saliency Maps: Saliency maps visualize the importance of each input feature by computing the gradient of the output $f(x)$ with respect to the input x :

$$\text{Saliency}(x_i) = \left| \frac{\partial f(x)}{\partial x_i} \right|.$$

SmoothGrad: SmoothGrad Smilkov et al. (2017) reduces noise in saliency maps by averaging gradients over multiple noisy samples of the input:

$$\text{SmoothGrad}(x) = \frac{1}{n} \sum_{i=1}^n \nabla_x f(x + \mathcal{N}(0, \sigma^2)).$$

Integrated Gradients: Integrated Gradients Sundararajan et al. (2017) attribute feature importance by integrating the gradients along the path from a baseline input x' to the actual input x :

$$\text{IG}_i(x) = (x_i - x'_i) \int_{\alpha=0}^1 \frac{\partial f(x' + \alpha(x - x'))}{\partial x_i} d\alpha.$$

Grad-CAM: Grad-CAM Selvaraju et al. (2019) generates heatmaps for convolutional neural networks by using gradients of the target output with respect to feature maps of a convolutional layer. For a given feature map A_k , the weights are computed as:

$$\alpha_k^c = \frac{1}{Z} \sum_i \sum_j \frac{\partial y^c}{\partial A_k^{ij}},$$

where y^c is the output score for class c , and Z is the spatial dimensions of A_k . The Grad-CAM heatmap is:

$$\text{Grad-CAM} = \text{ReLU} \left(\sum_k \alpha_k^c A_k \right).$$

Implementation Details for Section 6 & 7

We employ the off-the-shelf, publicly available implementations of the explainers from `Captum` library. (<https://captum.ai>). For (d)CKA, we utilized the publicly available package: `Simtorch` (<https://github.com/ykumards/simtorch>) with default (hyper)parameter selection. For Statistical testing with HSIC, we utilised the publicly available package: `PyRKHSstats` (<https://github.com/Black-Swan-ICL/PyRKHSstats>) with default (hyper)parameter selection except for the default p-value cutoff of 0.01. We have used p-value threshold of 0.05 throughout our experiments. In all our experiments, we considered the whole test set at once as a single batch for dCKA calculation and statistical testing with HSIC.

We run all our experiments on an NVIDIA DGX workstation, leveraging 1 Tesla V100 32GB GPU. We wrote all experiments in Python 3.10. Our total computational time for all experiments is roughly 81 hours.